Top Curr Chem (2010) 293: 207–258
DOI 10.1007/128_2009_8

Published online: 19 September 2009

Magnetic and Porous Molecule-Based Materials

Nans Roques, Veronica Mugnaini, and Jaume Veciana

Abstract In this chapter, we give an overview of the recent state-of-the-art research of porous and magnetic molecule-based materials. The subject is introduced by a section devoted to the fundamentals of magnetism in molecular magnets, with special attention to the design strategies to prepare molecular magnetic materials. We will then focus on the two main families of materials combining porosity and magnetism: the purely organic and the metal-organic porous magnetic materials. For both families, a selection of the most representative examples has been made. A complete section is devoted to magnetic and porous materials with flexible frameworks, an area of emerging importance in this field, because of their wide range of applications. Finally, we conclude with a brief overview on the most recent approaches for the future development of these materials.

Keywords Magnetism • Metal-organic frameworks • Open-shell organic molecules • Porosity • Purely-organic frameworks

Contents

N. Roques, V. Mugnaini, and J. Veciana (✉)
Institut de Ciencia de Materials de Barcelona (ICMAB-CSIC), Networking Research Center on Bioengineering, Biomaterials and Nanomedicine (CIBER-BBN), Campus Universitari de Bellaterra, E-08193, Cerdanyola, Spain
e-mail: vecianaj@icmab.es

N. Roques
CNRS ; LCC (Laboratoire de Chimie de Coordination) ; 205, route de Narbonne, F-31077 Toulouse, France
Université de Toulouse ; UPS, INPT ; LCC ; F-31077 Toulouse, France

1 Introduction

Since Flanigen and co-workers reported the synthesis of the first zeolite analogues – the microporous aluminophosphonate solids [1] – the number of synthetic porous solids has increased significantly. Over the past 30 years, in addition to the large number of porous phosphates described in the literature, new oxygen-containing porous materials have been obtained, combining phosphites, oxofluorides and oxochlorides, fluorides, nitrides, sulphates, sulphides, selenites, halides, germinates, arsenates, and cyanides with a large list of metal ions [2–4]. Together with the rapid development of these inorganic porous materials, a new class of porous solids emerged around 15 years ago, when organic molecules were introduced as direct constituents of porous structures. These porous solids result from the reaction between inorganic and organic species (the latter mainly containing O and/or N donor atoms) to build open-frameworks whose skeletons contain both organic and inorganic moieties mainly linked by strong bonds [5], at variance to supramolecular chemistry. According to the dimensionality of the inorganic framework, Férey classified these new porous materials into four different categories [6] (an alternative classification has been proposed by Cheetham and co-workers [7]) (Fig. 1). Thus, the introduction of organic connectors can induce pillaring between infinite inorganic 2-D layers or allow connecting infinite inorganic 1-D chains. These 2-D and 1-D systems are usually referred to as organic-inorganic hybrid materials, in contrast to the pure inorganic 3-D zeolites. Eventually, organic linkers could also be arranged around single ions or discrete polymetallic species, as in coordination chemistry, to afford 0-D structures, as far as the inorganic part is concerned. These 0-D inorganic structures will be referred from now on as coordination polymers or with the more general acronym MOFs (metal-organic frameworks).

Since the beginning of the 2000s, thousands of publications describing open-framework coordination polymers have been reported [8–15]. The reason why

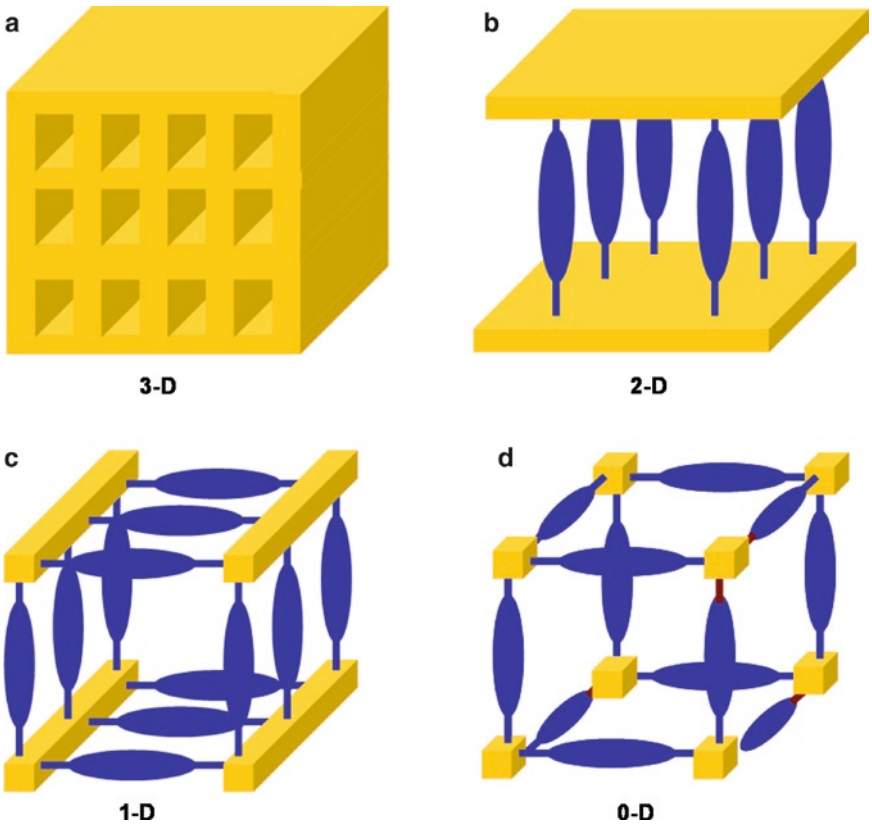

Fig. 1 Classification of porous structures depending on the dimensionality of the inorganic subnetwork. (**a**) 3-D pure "inorganic"-based framework; (**b**) Pillared 2-D "inorganic" layers through multitopic organic linkers; (**c**) 1-D "inorganic" chains linked through multitopic organic linkers; (**d**) Coordination polymers resulting from the connection of 0-D "inorganic" species (metal-organic assemblies or isolated metal ions) thanks to multitopic organic linkers. The design of this figure has been inspired from ref 6

these materials have attracted so much attention is twofold. First, and compared to "classical" porous solids, it consists in the potentiality offered by organic chemistry to design organic multitopic ligands combined with the huge number of metal ions and polynuclear species, previously isolated in coordination chemistry, providing an almost endless number of possibilities for creating new MOFs. Therefore, numerous examples of nanoporous coordination polymers have been reported in the last few years, showing diverse topologies, rigid or dynamic frameworks, increasingly higher pore sizes and specific surfaces, and various pore shapes and chemical nature [16]. The second reason is related to the important applications expected for these coordination polymers. As organic-inorganic zeolite analogues, these systems have shown relevant properties in the areas of ion exchange [17–22], separation processes, [23] and catalysis [24–26]. Particularly, their potential use in gas storage

applications [27–29] has greatly contributed to the expansion of this research line. For instance, Férey, Kitagawa, Yaghi, and co-workers have shown the ability of some MOFs in the sorption of carbon dioxide [30], methane [31–35], and hydrogen [27], domains of paramount importance concerning pollution and energy problems. Such results, together with the efficiency recently shown by some of these porous solids for industrial applications [36–39], make us think that MOFs-based gas storage devices will be developed in the near future. However, as far as properties are concerned, the major revolution comes from the large diversity of elements – metal ions or polynuclear species and organic molecules – involved in the direct composition of the open-framework. This situation opens new perspectives in the design of a second generation of multifunctional porous materials [40–42], which combine classical applications of zeolites associated to their inherent porosity character with the development of novel chemical and physical properties, such as, among others, magnetic, conductive, and/or optical properties (for a complete review on multifunctional open-framework materials see [43]).

Since magnetic open-framework materials are probably the most abundant among multifunctional porous materials reported to date, we aim to give, in this chapter, a short overview on the different types of magnetic and porous coordination polymers, although, due to the large number of examples so far described in the literature, we have decided to focus on representative cases. Therefore, in order to proceed in a pedagogic fashion, the second section will describe the main approaches used so far to construct molecule-based magnetic materials. Using the given information as a starting point, we will hence demonstrate, in the third and fourth sections, that the same tools and rules can be used to design magnetic and porous frameworks. Particularly, the third section will focus on purely organic open-frameworks, an emerging new class of porous solids composed of only organic molecules bonded by weak interactions, whose design takes advantage of supramolecular chemistry. The fourth section will be devoted to metal-organic coordination polymers and to some representative cases of MOFs. In the fifth section, we will show some cases reporting the most remarkable properties of coordination polymers: their dynamic structural transformations due to their flexible structures, which could be used to modulate the magnetic properties. Finally, the last section will be dedicated to the state-of-the-art research in this field, giving some representative examples on recent investigations focused on magnetic nanoporous materials.

2 Molecular Magnetic Materials: General Concepts

Magnetism has long attracted the imagination and attention of the scientific community, and magnets have been essential for the transformation of our society into the high-technology one of today [44]. Particularly, the remnance and hysteresis phenomena associated with magnetic materials are fascinating: hysteretic materials retain part of their magnetization and hence, can store information below their critical

temperature [45]. This characteristic explains the wide spreading study of molecule-based magnets for their application in modern technology as well as in the field of nanotechnology [46].

A magnetic material always consists of a spin-bearing moiety responsible for the magnetic behaviour. According to the nature of the spin site – also named magnetic unit – magnetic materials can be classified into traditional magnets, composed only of inorganic magnetic units, and molecule-based magnets, incorporating molecules in their structures. These latter ones will be the subject of this section [47].

A single spin-bearing moiety cannot be responsible for the magnetic character of a magnet, since magnetism is a bulk phenomenon, i.e., it is never associated with the presence of a single spin or many isolated spins, but rather with the presence of many interacting spins in bulk materials. Therefore, a magnet does not only consist in a magnetic unit, but also in a connector or spacer (either an organic or an inorganic species) able to propagate the magnetic interactions among the magnetic units. These connecting species can be either magnetically non-active or magnetically active. While magnetically non-active ligands are only responsible for the transmission of the exchange interactions by properly placing the spin-bearing sites in space, magnetically active spacers might play, in addition, an active role in the determination of the final magnetic properties of the material. A particular case is represented by pure organic magnets, where the magnetic unit is an organic open-shell molecule and the interaction between the spins is mediated by non-covalent bonds, such as hydrogen bonds, and therefore, no spacers, neither organic nor inorganic, are needed [48, 49], as will be described in Section 3. The main factors that contribute to the overall magnetic behaviour in molecule-based magnets are: (1) the topology of the molecules and (2) the molecular packing. The shape of the molecules and their electronic structure play a crucial role in determining the crystallographic structure, while the magnetic interaction or coupling between the spins through covalent and/or non-covalent bonds depends on the molecule packing that ultimately governs the cooperative behaviour. Hence, the molecular topology and the packing are of utmost importance for the interaction of the spins and the magnetic ordering at a characteristic temperature, named the critical temperature. Such a temperature will be determined by the strength of the magnetic interactions between the spins as well as by the dimensionality of such interactions. One of the goals of the research on molecular magnetism is to achieve a molecular material with a residual permanent magnetization at zero-field for an as-high-as-possible critical temperature, below which all spins of the magnetic units are ordered. The ordering of the spins may lead to three different types of cooperative magnetic behaviours: ferromagnetism, ferrimagnetism, and antiferromagnetism. In the case of ferromagnetism, the structure allows for a parallel alignment – ferromagnetic coupling – of all the spins in the ordered phase [50]. In both ferrimagnets and antiferromagnets there is an antiparallel alignment or antiferromagnetic coupling of the spins of neighbouring spin carriers. When the individual magnetic moments are different, the result is a non-zero total magnetic moment of the bulk material and the material is ferrimagnetic. Instead, when there is an antiparallel coupling of spins of identical magnetic moments, the magnetizations of the two sublattices cancel and

the material shows antiferromagnetism, with a total null magnetic moment. Since states of low-spin (LS) multiplicity are often more stable than states of high-spin (HS) multiplicity, and the structural and electronic requirements for achieving ferromagnetic couplings are much stricter than for antiferromagnetic ones, antiferro- and ferrimagnetism are much more common than ferromagnetism in nature.

2.1 Molecule-Based Magnetic Materials: Why?

Nowadays, research on molecule-based magnetic materials is focused on the study of molecular compounds, combining magnetic properties normally associated with inorganic materials with the chemical flexibility of their molecular tectons. While traditional inorganic materials, during their synthesis, are subjected to high temperatures, which ensure thermodynamic stability but limit chemical flexibility, one of the advantages provided by molecules is the possibility to alter and modulate the interactions between the building blocks, changing the structure of the molecule by means of organic chemical methods [51]. Moreover, if a multifunctional organic molecule is used as a synthon of the magnetic material, the result could be a multifunctional molecule-based magnetic material.

The increasing interest in molecular magnetism is explained not only by the larger malleability of molecular tectons but also by the large variety of possible applications of molecular magnetic materials into the emerging field of nanotechnology. Thus, molecular materials have emerged in many application areas such as data storage and quantum computation and the design of new conductors and superconductors, or novel non-lineal optical materials [44]. The presence of magnetism in such materials makes molecular magnetism even more interesting. Nevertheless, it remains a challenge to prepare a magnetic molecular material showing bistability at room temperature or above because of the difficulties in predicting not only the spatial arrangement of the molecules but also the strength of their magnetic interaction and hence, their bulk magnetic properties, which depend on both the architecture of the material and the cooperative intermolecular magnetic interactions.

2.2 Magnetic Interactions in Molecular Materials

The most interesting magnetic properties of a material are represented by ferromagnetism and ferrimagnetism, since they give rise to spontaneous magnetization below the critical temperature. Generally, the different behaviour of magnetic materials is explained on the basis of the magnetic exchange coupling, J, which describes the interaction between two spins and is defined by the effective spin Hamiltonian, $\hat{H} = -2JS_1S_2$, where $2J$ is the energy separation between the singlet and the triplet states. A positive J indicates ferromagnetic coupling, while a negative J indicates antiferromagnetic coupling. Generally, a parallel coupling between the spins occurs when the interacting magnetic orbitals are strictly orthogonal to each other, while if they have non-zero overlap, an antiparallel alignment will be favoured.

To have a bulk ferromagnet it is necessary that parallel couplings dominate along the three directions of the lattice, but the orthogonality conditions are difficult to impose on all the neighbours of a given spin at the same time, hence, making ferromagnetic behaviour a rarity. By contrast, antiferromagnetism is more common, since magnetic orbitals tend to overlap each other along the three directions of the lattice, favouring the antiparallel alignment of spins.

In the case of molecular materials, the first evidence of a purely organic compound with ferromagnetic interactions was given in the late 1960s when such interactions were identified in the case of galvinoxyl radicals [52] (Fig. 2).

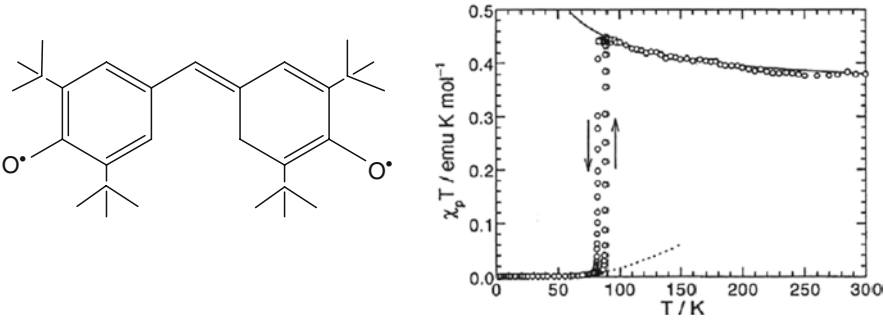

Fig. 2 Molecular formula (left) and magnetic susceptibility (right) of galvinoxyl radical. Reprinted from ref 52 [Blundell SJ, Pratt FL, "Organic and Molecular Magnets", (2004) J Phys Condens Matter 16:R771] with permission of IOP publishing Ltd

In the specific case of galvinoxyls, the small intermolecular SOMO–SOMO overlap, together with the excited charge transfer configurations, involving intermolecular interactions between the singly occupied molecular orbital (SOMO) on one molecule and the fully occupied molecular orbital on the other is responsible for the parallel alignment of the spins of neighbouring molecules. Thus, the small intermolecular SOMO–SOMO overlap can be considered as a requirement for ferromagnetic interactions in an organic compound, but only if the SOMOs are close enough for the electrostatic repulsion of neighbouring electrons to become effective [52]. Therefore, unpaired electrons interact ferromagnetically when the overlap integral is null or close to zero, a situation occurring for orthogonal orbitals, and when, at the same time, the exchange integral is significant [53]. Moreover, the propagation of the magnetic interactions along the three directions of the space depends strongly on the geometry of the molecule and its nature as well as on the type of packing forming the network of the solid.

2.3 Design Strategies for Molecular Magnetic Materials

Two different synthetic approaches to obtain molecule-based magnetic materials can be envisioned: (1) the organic approach and (2) the metal-organic approach. The first approach uses only organic molecules as magnetic units, i.e., organic free

radicals or radical-ions and no metallic ions, while in the second approach metal ions are always used as magnetic units.

2.3.1 Organic Approach

Organic radicals interacting through appropriate non-covalent bonds that allow the propagation of the magnetic interactions have been largely used as magnetic synthons following a methodology, herein called organic approach, which results in completely organic magnets. Functional groups attached to the skeleton of magnetic synthons may form supramolecular interactions that influence the solid-state structure and provide new pathways for intermolecular magnetic exchange interactions. According to the description given by Kahn in the late 1990s, magnetism is a "supramolecular function," related to the supramolecular interactions between spin-bearing molecules [54]. However, the interactions mediated by non-covalent bonds are generally very weak and extremely difficult to control. This limitation generally found for purely organic magnets is the reason why they are very rare. Moreover, their bulk magnetic order generally occurs only at very low temperatures. In purely organic magnets, the organic spin-bearing sites are open-shell molecules such as free radicals or radical ions. Most representative examples of radicals that show bulk magnetism are α-nitronyl nitroxide, verdazyl, and triphenylmethyl radicals (Fig. 3).

All these molecules share stability and persistency and take part neither in dimerization reactions nor in any other kind of addition reactions that could disrupt the presence of the unpaired electron. Moreover, the radical building blocks show enough persistency to assemble into crystalline structures where they remain isolated from one another and maintain their open-shell character.

According to the model described by McConnell, ferromagnetic interactions occur when the molecules closer in space have spin densities contacts of opposite sign [52, 55]. In contrast, antiferromagnetic interactions take place when a direct

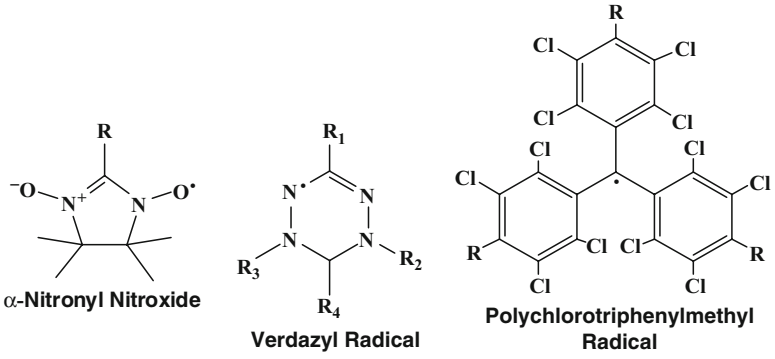

Fig. 3 Molecular formulas of the three families of stable radicals used as synthons to prepare molecular magnetic materials

overlap of the SOMOs of neighbouring molecules occurs. Because of that, the introduction of appropriate substituents into specific positions of the radical skeleton will change its packing motif, thus modifying the intermolecular magnetic exchange pathways and generating either ferromagnetic or antiferromagnetic interactions. One of the most efficient methods to modify intermolecular magnetic interactions is based on the use of hydrogen bonds, which provide a directional pathway for the transmission of magnetic interactions in several pre-established spatial directions [55, 56]. Consequently, they are the interaction of choice to design the final architecture of a material and hence, the nature and dimensionality of the magnetic interactions.

In the case of nitroxides and substituted nitroxides, the degree of delocalization of unpaired electron density is the key factor in controlling the resulting magnetic behaviour. Small changes can lead to significant modifications of the crystal structure, thereby altering the orbital overlaps and the magnetic interactions between unpaired spins on neighbouring molecules and hence, the bulk magnetic behaviour. To build organic magnets based on nitroxides, α-nitronyl nitroxides have been largely used as magnetic synthons. While in nitroxides such as TEMPO, the nitroxide group is isolated from the rest of the molecule, in α-nitronyl nitroxides there are two equivalent nitroxide groups whose unpaired electron is in a π* orbital. These are roughly equally localized onto the nitrogen and oxygen atoms, while the carbon atom located in-between the two nitroxide functions is a node in the SOMO (Fig. 4). Most of the spin density is located onto the ONCNO part of the five-membered ring, being positive in the NO groups and negative in the central C(sp^2) atom [53, 55, 57]. The α-nitronyl nitroxide radicals generally form 1-D or 2-D networks built by hydrogen bonds. The relative orientation of radicals depends on the position of the substituents on the nitroxide skeleton that rules the crystal packing and hence, the magnetic behaviour of the material.

Long-range ferromagnetism was reported for the first time by Kinoshita et al. [58, 59], the β-phase of *p*-nitrophenyl α-nitronyl nitroxide being the first example of a purely organic ferromagnet (Fig. 5) [60]. This compound was a seminal starting molecule to build organic ferromagnets that inspired the work of many researchers.

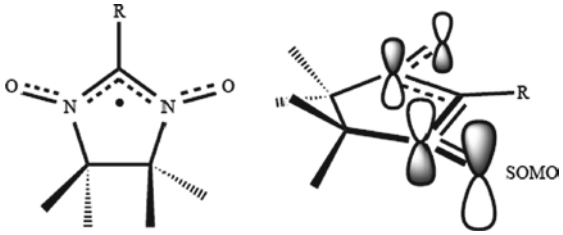

Fig. 4 General chemical structure of the family of α-nitronyl nitroxides and a representation of their singly occupied molecular orbitals (SOMO). Reprinted from ref. 55 [Amabilino DB, Cirujeda J, Veciana J, "Crystal architectures of organic molecular-based magnets", (1999) Phil Trans R Soc Lond A 357:2873] by permission of The Royal Society, Copyright 1999

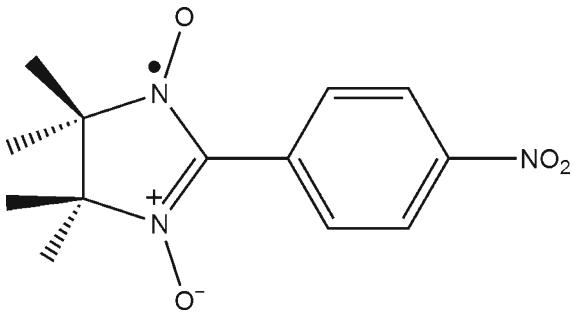

Fig. 5 Molecular formula of the *p*-nitrophenyl α-nitronyl nitroxide

Much effort has been spent on the investigation of the role of substituents and their position on the phenyl ring of α-nitronyl nitroxides [53]. The examples reported in the literature show that it has been possible to tune the magnetic interaction of α-nitronyl nitroxide-based materials by changing the type and position of the hydrogen bonding substituents that modify the crystal packing of the material. However, the extent of the magnetic interactions mediated through hydrogen bonds is quite low and hence, the critical temperature of these compounds is far from room temperature and below 4 K in most cases. Verdazyl radicals have also been investigated as tectons for molecule-based magnetic materials [61]. Their planar rings, together with the relative lack of bulky substituents and the presence of hydrogen bonding acceptor sites, make these radicals good candidates for the generation of magnetic materials [62]. Polychlorotriphenylmethyl (PTM) radicals were also successfully used for the preparation of purely organic magnetic materials, as will be reported in Section 3 [63].

2.3.2 The Metal-Organic Approach

Generally speaking, the so-called metal-organic approach consists of combining a magnetically active metal ion with an organic unit that acts as a polytopic ligand and in some cases may also be a spin-bearing unit. This strategy leads to magnetic materials with higher critical temperatures than purely organic magnets. Two main families can be distinguished. On one side are the magnets formed by magnetically active metal ions and organic moieties with a closed-shell electronic structure. In this case, the magnetic behaviour originates from the metal ion and the organic ligand has only a structural function promoting the magnetic interaction [52]. On the other side, magnets can also be formed by an organic ligand with an open-shell character combined with magnetically active metal ions. In the following subsections, we will summarize the most important aspects of both families of compounds that use the metal-organic approach.

Use of Closed-Shell Ligands

When using closed-shell ligands in the metal-organic approach, the organic moiety acts as polytopic ligand coordinating the metal ion, providing a good pathway for exchange coupling. By varying the nature, size, and the topicity of the ligand it is possible to prepare an infinite number of materials as well as tune their magnetic properties.

Many different compounds can be used as diamagnetic ligands with the role to space and transmit magnetic interactions. As it will be described in detail in Section 4.3.1, pyridine and pyrimidine derivatives can readily coordinate with metal ions and hence, give a MOF with generally weak magnetic character. However, pyridine derivatives (such as bipyridine) have been effective in the preparation of solids, showing both porosity and spin-crossover (SCO) phenomena. To increase the magnetic coupling between metal centres bearing unpaired electrons, shorter bridges – such as oxo, cyano, or azido – are usually needed. For example, the oxalate dianion (as will be shown in Section 4.1.2) is widely used as a bridging ligand to enable strong magnetic interactions between metallic centres when adopting the bidentate coordination mode. Acting as a rigid bidentate ligand, the oxalate dianion facilitates the formation of open-frameworks and modulates magnetic interactions. The role of the most representative linkers for the preparation of magnetic and porous coordination polymers will be discussed with examples in Section 4.

The most frequently used magnetic metal ions are of the transition series, but recently the world of lanthanides has also been investigated. These ions are attractive because, in some cases, they show magnetic anisotropy that renders them suitable to give bulk magnetism. Nevertheless, their lone electrons reside in the more internal *f* orbitals, resulting in magnetic interactions of one magnitude smaller than those involving transition metal ions. Another disadvantage of these ions is represented by the high coordination numbers, as compared to *d*-block transition metal ions, which may cause difficulty in controlling the synthetic reactions and thereby, the structures of the products [64].

Use of Organic Open-Shell Ligands

The methodology based on the use of a magnetic metal ion and an organic open-shell molecule, named the “metal-radical approach”, was originally introduced in the 1980s by the groups of Rey, Gatteschi and co-workers [50]. The leading idea is to combine the magnetic character of an organic radical ligand with a metal centre through coordination chemistry. Such units form a network of alternating stable radicals and metal ions, in which both constituents are generally antiferromagnetically coupled and have distinct magnetic moments, leading to a ferrimagnetic material [65]. The presence of the spin on both the metal ions and the radical represents an improvement in the magnetic properties with respect to those of closed-shell ligands with comparable sizes and, for this reason, is one of the most attractive strategies

for the design of molecule-based magnetic materials, especially if one wants to use large ligands generating open-framework structures. When metals and open-shell molecules are engaged in sufficiently strong exchange interactions, this approach leads to the preparation of networks with long-range magnetic order and high critical temperatures. The strength of magnetic interactions as well as the magnetic dimensionality of the molecular material are generally enhanced in comparison with that of systems made up from magnetic metal ions and closed-shell coordinating ligands [66]. The first requirement to build magnetic materials via the metal-radical approach is the availability of stable radicals able to coordinate or chelate the metal ions, and that can be easily modified allowing the design of multidimensional structures [67].

Nitrogen-based radicals like nitroxides and verdazyl derivatives fulfill the basic requirements, since they share high stability and persistency and can be functionalized to coordinate metal ions. Charged radicals such as tetracyanoethylene [68, 69] and tetracyanoquinone radical anions have also been reported [70], and a special case is represented by the *o*-quinone ligands that can be found in different oxidation states in valence tautomeric compounds [71]. Recently, PTM radicals substituted with carboxylate groups have been used to obtain metal-radical coordination polymers, which, in some cases, exhibit porous structures and relevant magnetic properties. Example of such porous magnets will be reported in detail in Section 4.3.3 [72].

3 Purely Organic Porous Magnetic Materials

As introduced in the previous section, different families of open-shell tectons have been used to prepare purely organic magnetic molecular materials following the organic approach. α-Nitronyl nitroxide derivatives, substituted with hydrogen bond donors to favour the packing and hence, the propagation of proper magnetic interactions, have been reported [53]. In these magnets, non-covalent hydrogen bonds play a key role in the magnetic behaviour, since they are responsible for the directional propagation of the magnetic interactions. However, the resulting coupling between the magnetic units is rather weak. For the second family of open-shell ligands, the verdazyl radicals, it has been reported how its small size, together with the planarity and π-stacking, results in strong magnetic exchange interactions, even when the two radical sites are quite far apart [61]. In all such examples, the organic tecton was a small molecule to transmit more effectively the magnetic interactions and consequently, the resulting material showed structure with close frameworks. However, as highlighted in the introductory part, the field of porous materials is of increasing interest due to its huge range of applications. So the question is: Is it possible to combine magnetic ordering and porosity in the same material? A positive answer was given by the preparation of purely organic open-frameworks showing magnetic properties using open-shell tectons with a trigonal symmetry [63]. The key point in this approach is the use of propeller-like trigonal free radicals, based

upon PTM structure, that are stable and persistent and that can be functionalized with a great variety of functional groups. The chemical stability of PTM radicals, due to the presence of six bulky chlorine atoms in the *ortho*-positions with respect to the central C-atom, makes them suitable organic magnetic units. The presence of the chlorine atoms is also responsible for the high localization onto the central sp^2 hybridized carbon atom of the electron spin density as well as for the twisting of the three phenyl rings, resulting in a propeller like structure of the radical. Even though PTM derivatives do not have a planar structure, and consequently, often show unpredictable packing, the rigidity and bulkiness of these open-shell molecules prevent in many cases their interpenetration, giving rise to solids with open-frameworks being one of the few examples of porous magnets. Thus, the introduction on the triphenyl methyl skeleton of groups capable of forming hydrogen bonds enables the formation of multidimensional interactions. Indeed, PTM radicals functionalized with several carboxylic groups are able to form robust and well-defined 2-D or 3-D frameworks that allow the propagation of weak ferromagnetic interactions [73, 74]. So far, four carboxylic -substituted PTM derivatives are available, named PTMMC, PTMDC, PTMTC, and PTMHC, according to the number of carboxylic functions (1, 2, 3, and 6, respectively), introduced onto the triphenylmethyl skeleton (Fig. 6).

The monocarboxylic PTMMC derivative does not form a rigid framework but gives an insight into the mechanism of the formation of intermolecular hydrogen bonds and transmission of magnetic interactions betwen bonded molecules in these fully chlorinated radicals [75]. PTMMC was synthesized and then crystallized following two different procedures that resulted in two phases, the α-phase and the β-phase. In the α-phase, obtained by diffusion of *n*-hexane into a dichloromethane solution of the radical, the PTMMC molecules associate into hydrogen-bonded centrosymmetric $[R_2^2(8)]$ dimeric synthons and show weak dominant ferromagnetic interactions. In the β-phase, obtained by slow evaporation of a radical solution in ethanol, the $[R_2^2(8)]$ dimeric synthons observed in the α-phase are disrupted by ethanol molecules. The ability of ethanol to form hydrogen bonds with the carboxylic groups of the radical leads to the disruption of any direct hydrogen bond between PTMMC radicals. In this phase, dominant antiferromagnetic interactions were found. The two different magnetic behaviours found in the α- and β-phase reveal that the propagation of ferromagnetic interaction mostly occurs through the

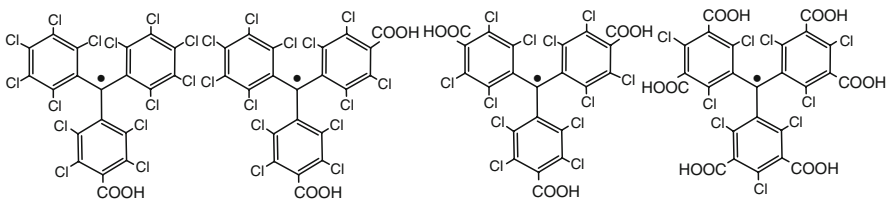

Fig. 6 Molecular formulas of the carboxy-substituted PTM derivatives (PTMMC, PTMDC, PTMTC, and PTMHC)

pathways defined by direct intermolecular hydrogen bonds between the carboxylic functions of PTM radicals.

Crystallization of PTMDC, following the same methodology used to obtain the α-phase of PTMMC, yields a robust extended hydrogen-bonded network named POROF-1, where POROF refers to pure organic radical open-framework. The presence of two carboxylic functions increases the dimensionality of the resulting structure and the intermolecular hydrogen-bonded connections between PTMDC radicals create a primary structure consisting of 2-D hydrogen-bonded sheets. Each molecule adopts two hydrogen-bonded motifs, the expected dimeric [$R_2^2(8)$] and the unusual hexameric [$R_6^6(24)$] unit, and these represent the repetitive units in POROF-1. The packing of the resultant 2-D layers creates an open-framework with 1-D channels, which are stable up to 275°C, even after the removal of included solvent molecules [76]. Magnetic measurements revealed weak antiferromagnetic interactions between the radical units at low temperature. In the case of the tricarboxylic PTM derivative, the presence of three carboxylic substituents allowed the preparation of a robust porous extended hydrogen-bonded 2-D network, POROF-2 [48, 49]. In POROF-2 , the repetitive unit is the hexameric [$R_6^6(24)$] motif, formed by six mutually hydrogen-bonded PTMTC molecules (Fig. 7a).

Each PTMTC molecule participates in the construction of three identical hexameric units that propagate along a plane (Fig. 7b). These 2-D layers stack through

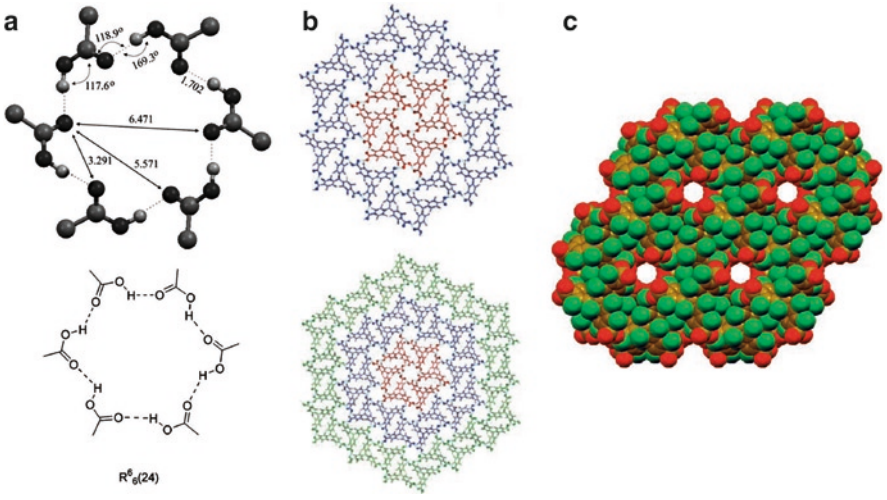

Fig. 7 (**a**) Geometrical characteristics of the hexameric [$R_6^6(24)$] ring formed by intermolecular hydrogen bonds of six PTMTC radicals. (**b**) Stepwise growth of the 2-D hydrogen-bonded sheets in POROF-2. (**c**) Space-filling representation showing the tubular channels. Reproduced with permission of ref 48 [Maspoch D, Domingo N, Roques N, Wurst K, Tejada J, Rovira C, Ruiz-Molina D, Veciana J, "Structural and Magnetic Modulation of a Purely Organic Open Framework by Selective Guest Inclusion" (2007) Chem Eur J 13:8153]. Copyright Wiley-VCH Verlag GmbH & Co. KGaA

Cl···Cl interactions and the resulting 3-D structure presents channels that can accommodate a sphere of 5.2 Å diameter (Fig. 7c). As for the magnetic properties, POROF-2 presents paramagnetic behaviour from 300 to 5 K, and a bulk ferromagnetic ordering below 2 K. It should be noted that POROF-2 is a unique example of a porous, purely organic structure, which shows long-range ferromagnetic ordering.

A PTM derivative with six carboxylic groups in the *meta* positions (PTMHC) forms 3-D hydrogen bonded open-framework. In this compound a solvent-free crystallization was not possible and mixtures of THF or diethyl ether and *n*-hexane were used. When using THF, the PTM hydrogen bonded network and thus, the transmission of the magnetic interactions are disrupted to yield a paramagnetic solid. However, when diethyl ether is used, the resulting crystal structure contains solvent molecules that only partially disrupt the expected 3-D hydrogen bonded structure. The resulting primary structure is formed by 2-D corrugated layers, with a $[R_6^6(48)]$ repetitive unit formed by six PTMHC molecules. For each molecule, three carboxylic groups are hydrogen bonded to solvent molecules, while the three remaining carboxylic groups interact with three other PTMHC molecules to give three identical hexameric units. The magnetic behaviour of this compound is very similar to that of POROF-2. Thus, in the range 20–300 K, this compound behaves as a paramagnet, and below 20 K, very weak intermolecular ferromagnetic interactions are present, and long-range magnetic ordering is expected at very low temperatures.

The availability of a family of carboxylic substituted organic open-shell compounds and the investigation of their magnetic properties allow some general observations on the behaviour of these radicals as synthons for magnetic materials: (1) increase in the number of carboxylic groups is accompanied by reduction of chlorine–chlorine contacts in the solid state; these latter contacts are usually responsible for antiferromagnetic interactions in this type of material; (2) the change in the position (*meta* versus *para*) of carboxylic groups does not appear to modify the ferromagnetic nature of the intermolecular magnetic interactions in the bulk material.

4 Metal-Organic Porous Magnetic Materials

Together with purely inorganic and molecular hybrid porous materials, coordination polymers, or 0-D zeotype systems, according to Férey's classification [6], have experienced a gigantic evolution along the last few years. Interest in this latter family of material is threefold when porosity and magnetism are combined in the same material. First, the huge versatility of molecular chemistry provides a large number of ligands whose shape and topology can be controlled. Second, and of paramount importance in the building of magnetic materials, these ligands have proven to provide good superexchange pathways. Finally, such materials may benefit from crystal engineering techniques to arrange, in a predictable fashion, transition metal ions or already identified polymetallic assemblies with organic or preformed metal-organic tectons.

In this section, we aim to give representative examples of magnetic and porous coordination polymers. We have selected examples that combine porosity and relevant magnetic properties, ranging from strong magnetic exchange interactions to magnetic ordering, to single-molecule magnet (SMM) behaviours. Since the efficiency of superexchange interactions between metal ions through bridging ligands is strongly related to the distance between the magnetic units and their relative orientation, the different examples have been divided into three subsections.

Section 4.1 will be devoted to porous and magnetic solids constructed around carboxylate-based ligands (O–C–O), which allow the formation of 1-D, 2-D or 3-D M–O–C–O–M and/or M–O–M subnetworks with magnetically active metal ions. In these systems, organic molecules are either small or extended polytopic ligands, but the magnetic properties are governed by the M–O–C–O–M or M–O–M structural motifs, which lead to strong interactions compared to the magnetic pathways defined by bridged metal ions through multitopic ligands. Section 4.2 will review examples of coordination polymers obtained by connecting metal-organic polymetallic species through polytopic organic ligands. In this class of polymers, magnetic properties are closely related to the magnetic properties of the "father" cluster and long-range magnetic ordering will only be observed if the organic ligands allow magnetic interactions between the polymetallic centres. Section 4.3 will deal with porous and magnetic coordination polymers where single ions are also connected through polytopic organic ligands. In this case, observation of magnetic properties for the bulk material will mainly depend on the distance separating the magnetic units and on the ability of the ligands to furnish efficient magnetic superexchange pathways between magnetically active metal ions.

4.1 Carboxylate-Based Porous Networks

A detailed review on carboxylate-based open-frameworks has been recently published [15]. As already mentioned, in order to obtain magnetic open-frameworks, the challenge is to control both pores size and chemical nature, together with the strength of magnetic interactions between spin-bearing moieties. In such a context, the use of short organic ligands, which favour the formation of 1-D, 2-D, and 3-D M–O–C–O–M and M–O–M carboxylate-based networks, will mediate strong magnetic interactions between magnetic units in 1-D, 2-D, and 3-D and yield, in some cases, open-framework architectures.

For this purpose, some of the most used ligands are formate (**1**), oxalate (**2**), malonate (**4**), succinate (**5**), fumarate (**6**), and glutarate (**7**) (Fig. 8). Oxamate-based ligands (**3**), inspired by the seminal work of Kahn and co-workers, have also attracted attention as nitrogen-containing oxalate analogues, since they tend to bridge metal ions not only through M–O–C–O–M but also through M–N–C–N–M motifs, which facilitate magnetic interactions. In this subsection, we include examples of magnetic porous solids constructed around the above ligands.

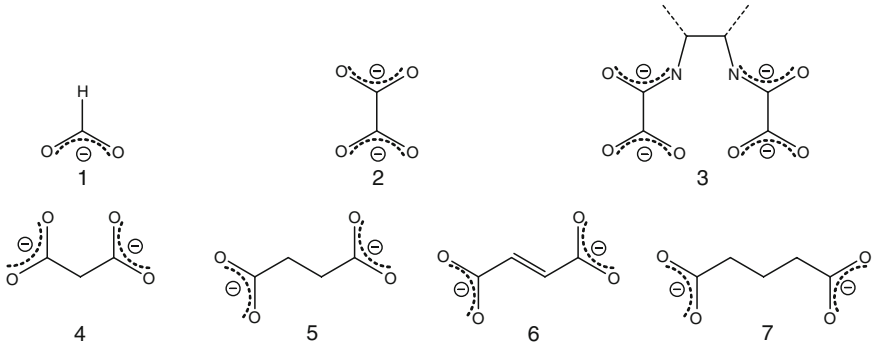

Fig. 8 Most used ligands to prepare coordination polymers with open-frameworks

4.1.1 Metal-Formate Networks

The formate ion (**1**) (Fig. 8) is the smallest and simplest carboxylate ligand, and has been widely used to prepare open-framework architectures showing high thermal stability even in the absence of guest solvent molecules [38]. The short $HCOO^-$ bridge is particularly efficient for the magnetic coupling between magnetically active metal ions. Moreover, the absence of any bulky substituent in **1** favours *anti–anti* coordination modes. Therefore, several magnetic open-framework metal formates showing 1-D, 2-D, and 3-D M–O–C–O–M/M–O–M subnetworks have been reported [77–81]. A representative example of this family of porous and magnetic solids is given by the compound $Mn_3(\mathbf{1})_6{\cdot}CH_3OH{\cdot}H_2O$, reported by Kobayashi, Kurmoo, and co-workers [82]. This solid possesses a diamondoid framework with high stability and flexibility for the inclusion of many types of guests. It exhibits 1-D channels with dimensions of 4 × 5 Å (32% of the total volume cell), where each node comprises $MnMn_4$ tetrahedral clusters built around a central Mn(II) ion, connected to four Mn(II) ions located at the apices via formate ligands to generate a 3-D M–O–C–O–M/M–O–M network. The network is robust up to 533 K and exhibits a particularly rich guest-modulated magnetic behaviour, as it will be explained in detail in Section 5.1. Both the as-synthesized and the evacuated solid show long-range magnetic ordering, with a critical temperature close to 8 K (Fig. 9).

Several additional examples of formate-based open-framework magnetic materials presenting long-range magnetic order have been reported. Depending on the metal ions used, the structural topology, the nature of guest molecules, and the use of ancillary ligands or ammonium templates, different kinds of magnetic ordering have been observed in the related materials, which order magnetically below temperatures ranging from 8 to 35.6 K [77–83]. Among them is the coordination polymer of formula $Mn(\mathbf{1})_3{\cdot}0.5CO_2{\cdot}0.25HCOOH{\cdot}0.75H_2O$, reported by Sessoli and co-workers, which shows particularly interesting porosity and traps CO_2 molecules in its cavities [83].

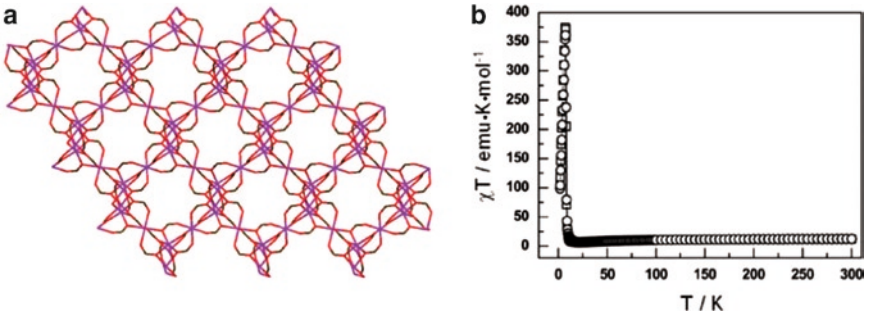

Fig. 9 (**a**) Structure of evacuated $[Mn_3(\mathbf{1})_6]$ showing the 1-D channels. (Mn, *purple*; O, *red*; C, *brown*). (**b**) Temperature dependence of the χ•T product for an applied magnetic field of 100 Oe. Reproduced from ref. 82 by permission of The Royal Society of Chemistry. http://dx.doi.org/10.1039/b314221c

4.1.2 Metal-Oxalate Networks

As in the case of formate, the dicarboxylate oxalate ion (**2**) (Fig. 8), which acts as a rigid ambidendate ligand, facilitates the formation of open-framework coordination polymers and mediates the magnetic interactions between magnetic metal ions through similar "inorganic" M–O–C–O–M or M–O–M subnetworks. So far, the use of such a ligand has led to several examples of mixed-valence polymers with 2-D and 3-D open-framework architectures, respectively. In the first case, the 2-D coordination polymers are described with the common formula $(A)\cdot[M^{II}M^{III}(\mathbf{2})_3]$, where A can be an ammonium, an alkali-metal, or a bis-cyclopentadienyl M(III) complex such as $[Cp_2M^{III}]^+$ [84–92]. Overall, the crystal structure shows a templated framework formed by alternating M(II) and M(III) metal ions through oxalate ligands in a 2-D honeycomb-like lattice, the positively-charged species being located in the channels resulting from the packing of the different layers (Fig. 10a). Various formulae are observed for 3-D MOFs resulting from the oxalate coordination chemistry: $[M_2^{II}(\mathbf{2})_3]$, $[M^{I}M^{III}(\mathbf{2})_3]$ and $[M^{II}M^{III}(\mathbf{2})_3]$ [93–95]. These compounds are based on an oxalate-bridged (10,3)-chiral network able to host in its 1-D channels cationic metal complexes such as $[M^{II}(2,2'\text{-bpy})_2]^{2+}$ (2,2'-bpy = 2,2'-bipyridine) (Fig. 10b).

The wide range of possible combinations of M(II) and M(III) magnetically active metal ions afford long-range anti-, ferro- and ferrimagnetic behaviours [96–99]. Depending on the material, magnetic ordering temperatures range from 8 K up to 70 K. However, the main drawback of oxalate-based frameworks is related to the presence of cationic species within their channels, since their removal or exchange leads to the collapse of the open-framework. To date, and to the best of our knowledge, the only exception is $Na_2(N(CH_3)_3Ph)_5[Cr(\mathbf{2})_3]_2Cl\cdot 5H_2O$, which maintains its structure on cation exchange or partial thermal removal of the template [100].

The possibility to combine several physical properties in the same molecular material has greatly contributed to the development of this family of coordination polymers. Added to the already mentioned chiral characteristics presented by some

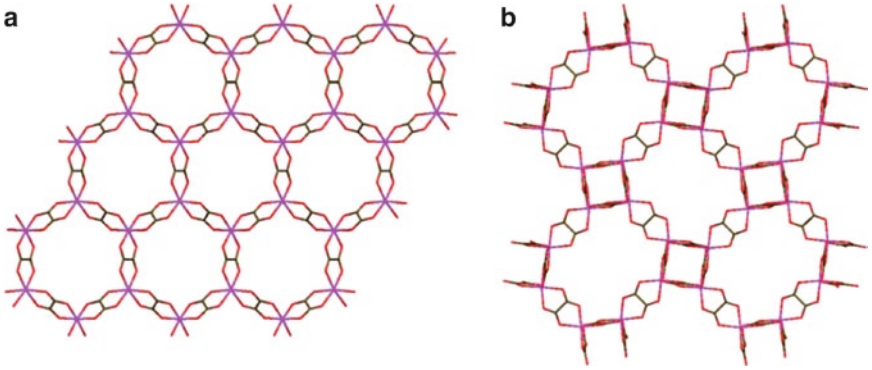

Fig. 10 Projection of the two representative templated lattices constructed from using oxalate ligands. (**a**) 2-D honeycomb framework of (A)•[M(II)M(III)(**2**)$_3$] (where A refers to ammonium cations, alkali-metal cations, or $Cp_2M(III)$). (**b**) Chiral (10,3)-network observed in [M(II)$_2$(**2**)$_3$], [M(I)M(III)(**2**)$_3$], and [M(II)M(III)(**2**)$_3$]. (M, *purple*; O, *red*; C, *brown*. Cationic templates are omitted for clarity). Adapted from ref 43 [Maspoch D, Ruiz-molina D, Veciana J (2007) Chem Soc Rev 36:770, "Old materials with new tricks: multifunctional open-framework materials"] by permission of The Royal Society of Chemistry, http://dx.doi.org/ 10.1039/b501600m

of these solids and interest in the quest for optically active molecular materials [101, 102], a strategy based on functional cationic templates has also been successfully developed. For instance, Coronado and co-workers have reported a series of magnetic conductors using tetrathiafulvalene (TTF) radical cations as cationic counterparts [103, 104]. A representative example of this is given by the material [BEDT-TTF]$_3$ [MnCr(**2**)$_3$], where BEDT-TTF stands for bis(ethylenedithio)TTF, which alternates magnetic oxalate-based anionic layers with conductive positively-charged BEDT-TTF. This molecular solid behaves as a magnet below 5.5 K and is metallic down to at least 0.2 K [105].

In the race to obtain molecular materials showing robust structures and higher magnetic ordering temperatures, two more examples have to be highlighted before closing this subsection. Related to the structure robustness, Li and co-workers reported a series of coordination polymers of general formula [M^{II}(**2**)(4,4'-bpy)]$_n$ (M = Fe, Co, Ni) [106, 107]. These solids result from the linkage of metal-oxalate chains through 4,4'-bipyridine ancillary ligands, and show rectangular-shape channels with dimensions of 5 × 8 Å and are stable up to 563–613 K. Furthermore, magnetic properties revealed a spontaneous antiferromagnetic ordering with transition temperatures of 12, 13, and 26 K for the Fe-, Co-, and Ni-based materials, respectively. These results are attributed to the combination of both the strong magnetic exchanges within the 1-D metal-oxamate chains and the weaker ones mediated through the bipyridine connectors.

Julve, Lloret, and co-workers have reported several isomorphous oxalate-based coordination polymers presenting magnet behaviour through spin canting below 40 and 70 K [108, 109]. Among them, the 3-D and chiral coordination polymer [Fe$_2$(**2**)$_2$(OH)Cl$_2$]·EtNH$_3$·2H$_2$O is the most interesting. This material possesses helical

channels (ca. 12 × 6 Å), in which the alkyl ammonium and water molecules are associated through hydrogen bonds. The structure is constructed around Fe(II)-oxalate chains interconnected through hydroxo-bridges. Remarkably, this coordination polymer undergoes a non-reversible solid–solid transformation together with a colour change when the crystals are exposed to air. In this transformation, a proton transfer occurs between the hydroxo bridge and one of the host water molecules, thus forming a new compound *o*[Fe_2(**2**)$_2$(O)Cl_2]·$EtNH_3$·H_3O·H_2O. Even though this transformation leads to a decrease in channel symmetry, the new solid still behaves like a magnet below 70 K [109].

4.1.3 Metal-Oxamate Networks

Like their fully oxygenated analogues, oxamate-based ligands (**3**) (Fig. 8) have also gained much attention in the field of molecular magnetism, and some of the first examples of molecule-based magnets were obtained following the rational-design strategy developed by Kahn and co-workers. In this pioneering work, mononuclear oxamato copper(II) complexes [Cu(**3**)]$^{2-}$ were used as bis(bidentate) metallo-ligands toward fully solvated metal ions to form heterobimetallic 1-D coordination polymers through M–O–C–O–M and M–N–C–N–M repeat units. Depending on the interchain interactions, the ferrimagnetic chains [M^{II}Cu(**3**)] (M = Mn, Fe, Co, Ni) show either ferromagnetic (T_C = 4.6–9 K) [110–113] or antiferromagnetic order (T_N = 2.4–3 K) [113, 114]. In subsequent work, Kahn, Stumpf, and co-workers prepared the corresponding oxamato-bridged $M_2^{II}Cu_3$ 2-D planar species (M = Mn, Fe, Co, Ni) presenting either an open-framework structure or a perpendicular interlocked disposition of honeycomb hexagonal planes depending on the nature of the counter-cation, which could be an alkaline [115] or an alkylammonium [116–118] cation as in the case of oxalate-based networks, or even a substituted pyridinium derivative of nitronyl nitroxide [119–122]. Unlike their 1-D analogues, these compounds have a higher ordering temperature, with T_C values up to 37 K. These examples perfectly illustrate the influence of the structural dimensionality upon the magnetic ordering temperature. Moreover, the change in anisotropy of the incorporated metal ion plays a fundamental role. Generally, Mn_2Cu_3 planes behave as soft magnets (H_c = 10 Oe) [116, 117, 119], whereas Co_2Cu_3 ones are hard magnets (H_c = 25 Oe) [121]. This is due to the large differences in magnetic anisotropy, with Co(II) ions being highly anisotropic and Mn(II), isotropic. Inspired by this work, Julve, Lloret, and Journaux extended this well-known "complex as ligand" approach by using oligonuclear complexes of late first row transition metal ion, from mono- to trinuclear, working with related aromatic-substituted mono-, di-, and tri-oxamate-based molecules (**8–10**) as ligands (Fig. 11) (for a detailed review on this strategy, see [123]).

This strategy was particularly elegant, since the reaction between the oxamate ligands with metal ions afforded pre-defined metallotectons. For example, coordination of Cu(II) through the bidentate N,O-oxamate donor set of **8** was aimed to afford the linear, ditopic metallotecton [Cu^{II}(**8**)]$^{2-}$, while reaction of the same

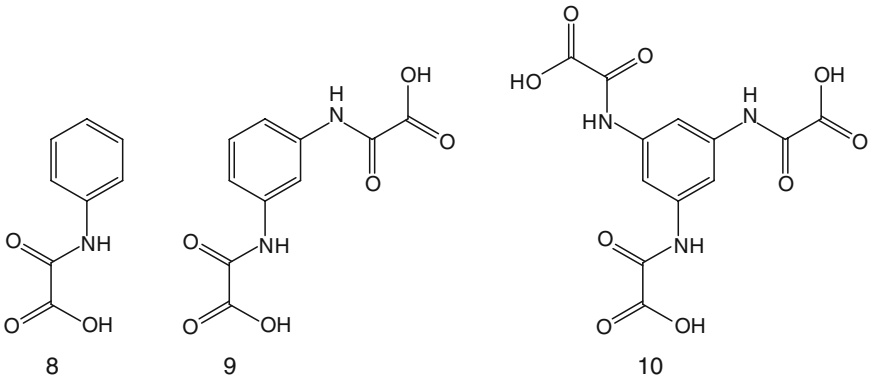

Fig. 11 Aromatic-substituted mono-, di-, and tri-oxamate-based molecules used as polytopic ligands

molecule with Ni(II) or Co(II) targeted the trigonal and tritopic building blocks $[Ni^{II}(\mathbf{8})]^{4-}$ and $[Co^{II}(\mathbf{8})]^{4-}$, respectively. Mono-, di-, tri-, hexa-, octa-, and nonanuclear complexes were prepared via blocking the outer *cis* carbonyl-oxygen atoms of the oxamate groups with well-known nitrogen-based metallamacrocycles stoppers. Careful magneto-structural correlations on metallotectons involving ligands **9** or **10** confirmed that the weak intramolecular interactions mediated through the *meta*-substituted phenyl rings are ferromagnetic and could be masked by the intermolecular antiferromagnetic interactions and/or magnetic anisotropy effects. On this basis, the already identified H-shaped metallo-ligand $[Cu^{II}(\mathbf{9})]^{4-}$ an its methylated analogue $[Cu^{II}(\mathbf{Me_3}\text{-}\mathbf{9})]^{4-}$ were reacted with Co(II) to afford the neutral heterobimetallic 2-D coordination polymers $[Co_2^{II}Cu_2^{II}(\mathbf{9})_2(H_2O)_6]\cdot 6H_2O$ and $[Co_2^{II}Cu_2^{II}(\mathbf{Me_3}\text{-}\mathbf{9})_2(H_2O)_6]\cdot 6H_2O$ (Fig. 12). The crystal structure of $[Co_2^{II}Cu_2^{II}(\mathbf{9})_2(H_2O)_6]\cdot 6H_2O$ shows a brick-wall 2-D architecture of (6,3) net topology [124]. In these isostructural solids, each $Co_2^{II}Cu_2^{II}$ rectangular corrugated layer is made up of oxamato-bridged $Co^{II}Cu^{II}$ linear chains running parallel to the *a*-axis, which is further connected through two *m*-phenylenediamidate bridges between the Cu(II) ions to give binuclear metallacyclic cores of the cyclophane-type, which define the short edge of the rectangle. The adjacent planes stack above each other to give an infinite array of interdigitated layers along the *b*-axis. This packing is mediated through weak hydrogen bonds and the neighbouring layers are displaced in a parallel manner along the *a*-axis: As a consequence, small square pores that are occupied by hydrogen bonded crystallization water molecules are formed.

In this series of metallacyclophane-based $Co_2^{II}Cu_2^{II}$ layered compounds, the double *meta*-substituted phenylene linkers ensure a ferromagnetic interaction between the oxamato-bridged ferrimagnetic chains. Hence, the complex $[Co_2^{II}Cu_2^{II}(\mathbf{9})_2(H_2O)_6]\cdot 6H_2O$ behaves as a metamagnet, with a long-range 3-D antiferromagnetic ordering ($T_N = 8.5$ K) and a ferromagnetic-like transition at a critical field of 1.2 kOe, which is sufficient to overcome the weak interlayer antiferromagnetic interactions. In contrast, the complex

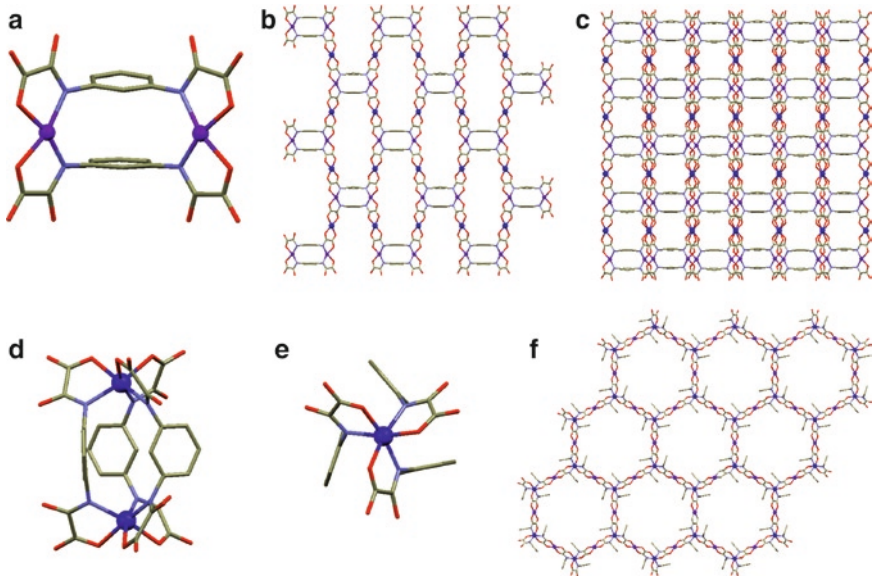

Fig. 12 "Metal-oxamate" approach for coordination polymers $Co(II)_2Cu(II)_2(\mathbf{9})_2(H_2O)_6 \bullet 6H_2O$ (A-C) and $Li_5[Li_3M(II)_2\mathbf{9}_3\ (H_2O)_6] \bullet 31H_2O$ (M = Ni and Co) (**d-f**). (**a**) H-shape metallo-ligand $Cu(II)(\mathbf{9})^{4-}$. (**b**) Corrugated layer resulting from the reaction of the H-shape metallo-ligand with Co(II) ions. (**c**) Packing of the corrugated layers showing square-like channels running along the *b*-direction. *Side* (**d**) and *top* (**e**) view of the hexatopic metallo-ligand $[M(II)_2\mathbf{9}_3]^{8-}$ (M = Ni or Co). (**e**) Reaction of hexatopic metallo-ligands with Li^+ or Mn^{2+} metal ions afford a 3-D honeycomb architecture of (6,4) net topology with large channels running along the *c* direction. (From (**a**) to (**c**): Cu, *purple*; Co, *blue*. From (**d**) to (**e**): Co or Ni, *blue*; Li or Mn, *purple*. In all cases: O, *red*; C, *brown*, N, *light blue*. Cationic templates and water molecules are omitted for clarity) (the figure design has been inspired from refs 124 and 125)

$[Co_2^{II}Cu_2^{II}(\mathbf{Me_3\text{-}9})_2(H_2O)_6]\cdot 6H_2O$ shows a long-range (most likely 2-D) ferromagnetic order at $T_C = 24.0$ K because of the minimization of the interlayer magnetic interactions that would lead to well-isolated planes of Ising-type magnetic anisotropy. The differences observed between the two coordination polymers in the magnetic ordering are attributed to the presence of the methyl substituents on the ligands, which, in the second case, tend to separate the planes from each other, thus weakening the interlayer interactions.

Very recently, a series of isostructural 3-D open-framework architectures have been obtained following a comparable approach. In this case, the dinickel(II) and dicobalt(II) complexes $[M_2^{II}(\mathbf{9})_3]^{8-}$ act as hexatopic ligands toward fully solvated Li^+ or Mn^{2+} ions to give anionic heterobimetallic 3-D compounds of general formula $[Li_3M_2^{II}(\mathbf{9})_3(H_2O)_6]_n^{5n-}$ and $[Mn_3M_2^{II}(\mathbf{9})_3(H_2O)_6]_n^{2n-}$, respectively [125]. The crystal structures of the lithium salts $Li_5[Li_3M_2^{II}(\mathbf{9})_3(H_2O)_6]\cdot 31H_2O$ (M = Ni, Co) show a 3-D honeycomb architecture of (6,4) net topology. The crystal lattice of these two isostructural compounds consists of an infinite parallel array of anionic

oxamate-bridged $Li_3M_2^{II}$ hexagonal layers growing in the *ab* plane; the adjacent layers are interconnected through three *m*-phenylenediamidate bridges between the M(II) ions to give binuclear metallacryptand cores of the meso-helicate-type, which act as pillars of the hexagonal prismatic structure. Overall, this leads to an open-framework structure showing hexagonal pores of ca. 22.5 Å in diameter (along the *c*-direction), where hydrogen bonded water crystallization molecules and solvated Li^+ species $[Li(H_2O)_6]^+$ are located. The magnetic properties of this family of metallacryptand-based $M_3^IM_2^{II}$ open-framework compounds depend mainly on the diamagnetic or paramagnetic nature of M(I) and on the magnetic anisotropy of M(II). Hence, the compounds $Li_5[Li_3M_2^{II}(\mathbf{9})_3(H_2O)_6]\cdot 31H_2O$ (M = Ni, Co) behave as isolated M_2^{II} complexes with weak ferromagnetic interactions between the M(II) ions (M = Ni, Co) across the three *meta*-substituted phenylenediamidate bridges within the metallacryptand core [J = +3.2 (M = Ni) and +1.0 cm^{-1} (M = Co)]. Similarly, the three *meta*-substituted phenylene linkers ensure a ferromagnetic interaction between the oxamato-bridged ferrimagnetic planes in the compounds $Li_2[Mn_3M_2^{II}(\mathbf{9})_3(H_2O)_6]\cdot 22H_2O$ (M = Ni, Co), which lead to a long-range 3-D ferromagnetic order at T_C = 6.5 K for both of them.

4.1.4 Fumarate-, Glutarate-, Malonate-, and Succinate-Based Networks

Numerous examples of metal channel-like magnetic complexes synthesized using malonate (**4**), succinate (**5**), fumarate (**6**), and glutarate (**7**) ligands (Fig. 8) have been reported. For most of these porous solids, a 3-D framework is obtained by connecting 2-D carboxylate-based layers with bifunctional ligands, the same ligands also acting as pillars [126–132]. This topology usually defines 1-D channels running parallel to the layers. However, from a magnetic point of view, these solids rarely show long-range magnetic ordering. An exception to this topology was found in the malonate complex [Cu(**4**)(DMF)], which shows a 3-D chiral diamond-like open-framework resulting from the connection of Cu(II) ions through malonate linkers and behaves as a ferromagnet below 2.6 K [133].

Especially attractive from a magnetic point of view are the open-frameworks involving infinite M–O–M type linkages. For example, Forster and Cheetham have described a nickel succinate $[Ni_7(\mathbf{5})_6(OH)_2(H_2O)_2]\cdot 2H_2O$ with infinite Ni–O–Ni connectivity, and exhibiting 1-D hydrophobic channels composed of large cavities of dimensions of 8 Å and narrower apertures of 4 Å [134]. This material exhibits a high thermal stability up to 673 K and may be magnetically frustrated. Similarly, the nickel glutarate $[Ni_{20}(\mathbf{7})_{20}(H_2O)_8]\cdot 40H_2O$ reported by Guillou et al. presents an infinite Ni–O–Ni connectivity with very large intersecting 20-membered ring channels and a pure ferromagnetic ordering at 4 K [135]. The porosity characteristics of this material are particularly interesting, since it can be dehydrated at 423 K and slowly rehydrated under air at room temperature, and when the sample is activated at 473 K shows a surface area of 346 $m^2\cdot g^{-1}$. Also, an open-framework showing ferrimagnetic behaviour below 20 K has been prepared by the same authors using succinate (**5**) ligands. The porous solid $[Ni_7(\mathbf{5})_4(OH)_6(H_2O)_3]\cdot 40H_2O$ shows 1-D

connected Ni–O–Ni chains and presents a reversible dehydration/hydration process, with a specific surface of 135 $m^2 \cdot g^{-1}$ for its activated form [136].

4.2 *Networks Based on Metal-Organic Polynuclear Species and Polytopic Organic Ligands*

So far, most part of the porous and magnetic coordination polymers we have described are constructed around 1-D, 2-D, or 3-D "inorganic" subnetworks. However, discrete di-, tri-, tetranuclear, and higher nuclearity metal-organic assemblies, such as the carboxylate-based paddle-wheel copper acetate and trimeric zinc or iron acetates are suitable building blocks – commonly called secondary building block units (SBUs) - for polymerization reactions involving polytopic ligands [10]. Such clusters are spaced in defined geometries depending on their own geometry and the geometry of the polytopic ligands. As a result, extended coordination polymers with high porosity and predictable structures are typically obtained. Using a cluster with an inherent property, one can then imagine distributing these SBUs in a desired way along the 3-D of space to create porous solids with novel functionalities. For example, catalytic clusters may be included in the skeleton of a porous structure, increasing the accessibility for these units and, therefore, enhancing their catalytic properties. From the magnetic point of view, the assembly of clusters also provides an excellent route to magnetic porous solids. The advantages of this strategy are obvious, since on one hand larger pores can be obtained from large cluster units and, on the other, the functional framework inherits the interesting physical properties derived from the clusters. However, since magnetic properties in the bulk are resulting from cooperative effects, the ligands used have to allow the establishment of magnetic interactions between the magnetically active SBUs, while the magnetic interactions between the metal ions within the SBU will also greatly influence the overall magnetic behaviour. This subsection gives a few representative examples of porous and coordination polymers constructed around metal-organic SBUs, starting with high nuclearity species, and then, examples of magnetic MOFs constructed around more common low nuclearity metal-organic clusters.

4.2.1 High Nuclearity Metal-Organic SBUs

Despite the numerous examples of high nuclearity metal-organic clusters presenting SMM behaviour reported in the literature since the beginning of the nineties, only a few examples of multidimensional coordination polymers using such clusters as SBUs behaving as SMMs have been described [137–140]. These systems are based upon the assembly of SMM acting as SBUs, thanks to coordination bonds [137], diamagnetic metal ions [138], and/or hydrogen bonds [139]. Among them, the isostructural coordination polymers of formula $\{[Mn_{19}Na(\mu_4\text{-}O)_9(\mu_3\text{-}O)(\mu_3\text{-}OH)_3(O_2$

$CMe)_9(pd)_9(H_2O)_3][OH]\}_n$ and $\{[Mn_{19}Na(\mu_4\text{-}O)_9(\mu_3\text{-}O)(\mu_3\text{-}OH)_3(O_2CMe)_9(mpd)_9(H_2O)_3][OH]\}_n$ (pd = propanediolate, mpd = 2-methyl-propanediolate) reported by Christou and co-workers [140] are the only ones that show an open-framework architecture. In these coordination polymers, the structure is constructed around the Mn_{19} SBUs containing seven Mn(II) and 12 Mn(III) ions. The manganese–oxygen core of each SBU consists of three equilateral triangles stacked one above the other. The basal triangle contains ten manganese ions, nine at its edges and the tenth near its centre, whereas the middle and apex triangles contain six and three manganese ions, respectively, all of which lie on their edges. The manganese ions of the core are held together by nine $\mu_4\text{-}O^{2-}$, one $\mu_3\text{-}O^{2-}$, and three $\mu_3\text{-}OH^-$ ions, resulting in an overall triangular-pyramidal frustum topology. The peripheral ligation is completed by nine bridging propanediolate ligands, nine bridging O_2CMe^- ligands, and three terminal H_2O molecules. Each Mn_{19} aggregate is connected through three $\mu_3\text{-}O_2CMe^-$ ligands to a Na^+ ion, while these SBUs are also directly interconnected through $\mu_3\text{-}O_2CMe^-$ ligands. Examination of the two structures reveals highly ordered 3-D structures that contain large rectangular channels with dimensions of approximately 12 × 16 Å (Fig. 13a). These channels are nearly empty, containing only a very small proportion of H_2O molecules and OH^- counterions, and originate a void space of approximately 44%. The SMM behaviour of these extended systems was confirmed, thanks to magnetisation versus dc field measurements. Below 1.1 K, they show magnetic hysteresis loops and their coercivity increases with decreasing temperature (Fig. 13b).

Besides these two examples, a series of open-framework architectures showing rather weak antiferromagnetic interactions have also been constructed around Ln_7 [141] and Mn_6 [142, 143] SBUs. In the latter SBU, the 3-D coordination polymer

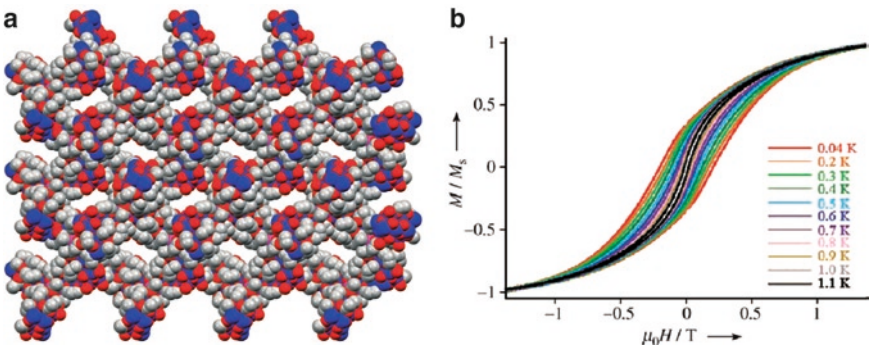

Fig. 13 (**a**) Space filling representation (along the *c* axis) for the polymeric structure of $\{[Mn_{19}Na(\mu_4\text{-}O)_9(\mu_3\text{-}O)(\mu_3\text{-}OH)_3(O_2CMe)_9(pd)_9(H_2O)_3][OH]\}_n$ showing the large channels (Na, *pink*; Mn, *blue*; O, *red*; C, *grey*; OH^- anions and water molecules are omitted for clarity). (**b**) Field dependence of the magnetization (hysteresis loop) for single crystals of the same solid at the indicated temperatures; the magnetization (*M*) is normalized to its saturation value. Reproduced with permission of ref 140 [Moushi EE, Stamatatos TC, Wernsdorfer W, Nastopoulos V, Christou G, Tasiopoulos AJ "A Family of 3D Coordination Polymers Composed of Mn19 Magnetic Units" (2006) Angew Chem Int Ed 45:7722]. Copyright Wiley-VCH Verlag GmbH & Co. KGaA

reported by Ovcharenko et al. in 2004 perfectly illustrates the difficulty in obtaining relevant magnetic properties in the final solid [143]. Substitution of preformed $[Mn_6(O_2)Piv_{10}]$ (piv = pivaloate) afforded magnetic clusters linked through magnetically active α-nitronyl nitroxide ditopic ligands. This coordination polymer has a 3-D open-framework diamond-like structure and shows the onset of weak antiferromagnetic interactions at low temperatures.

4.2.2 Tetra- and Trinuclear Metal-Organic SBUs

Tetra- and trinuclear SBUs have also been reported as constituents of porous and magnetic coordination polymers. Coordination polymers constructed around Co_4 [144] and cubane-like Ln_4 [145] assemblies have been reported, and these systems present contrasting porosity and robustness, but show only weak and predominant antiferromagnetic interactions at low temperature. Very recently, Yang and co-workers described a series of 3-D lanthanide-transition MOFs constructed around two distinct tetranuclear units of Ln_4 cubanes and chair-like Cu_4 clusters [146].

More interesting from a magnetic point of view is the porous coordination polymer reported by Wu and co-workers [147]. This solid is built from tetranuclear Co(II) citrate clusters as octahedral linkers and Co(II) ions as trigonal nodes. This connectivity shows an anatase topology with channels of 9.5 × 4.3 Å along two directions, leading to an apparent Langmuir surface area of 939 $m^2 \cdot g^{-1}$ and a pore volume of 0.31 $cm^3 \cdot g^{-1}$. This material behaves as a 3-D canted antiferromagnet with a magnetic hysteresis loop observed at 2 K.

Trinuclear metal-organic building blocks, such as Cr_3 or Fe_3 containing assemblies, have been used by Férey and co-workers to build highly porous and robust coordination polymers [30]. An example of an MOF-based trimeric structural unit was described by Barthelet et al. [148]: the coordination polymer $[V^{III}(H_2O)]_3O(C_8O_4H_4)_3(Cl \cdot 9H_2O)$ exhibits a 3-D framework built from octahedral vanadium trimers, joined via isophthalate anionic linkers to delimit cages where water molecules and chlorine ions are occluded. Although the trimeric clusters are connected along three directions, the 120° triangular topology of V(III) ions in each cluster induces a spin-frustration of their magnetic moments and therefore, a lowering of the temperature for magnetic ordering.

4.2.3 Binuclear Metal-Organic SBUs

One of the most frequently used SBUs is the binuclear paddle-wheel copper (II) dimer. In this motif, the two copper ions are strongly interacting in an antiferromagnetic fashion. This dimeric building-block supplies a square planar building block with four grafting sites, therefore, its connection provides coordination polymers combining relevant magnetic properties with contrasted porosity by an appropriate choice of ligands.

In 1999, Williams and co-workers were the first to report the magnetic properties of a porous structure based on the connectivity of paddle-wheel Cu(II) dimers through 1,3,5-benzenetricarboxylate ligands (BTC), with a 3-D structure with formula $[Cu_3(BTC)_2(H_2O)_3]$, referred to as HKUST-1[149, 150]. The connectivity between square planar copper-based SBUs and trigonal organic ligands afford a 3-D network showing channels with fourfold symmetry and a diameter of 9 Å. In addition, the structure remains crystalline up to 513 K. Water molecules that fill the channels can be readily removed at 373 K without a loss of structural integrity. Resulting voids give a surface area of 917.6 $m^2 \cdot g^{-1}$, a calculated density of 1.22 $g \cdot m^3$, and an accessible porosity of nearly 41% of the total volume cell. Interestingly, additional experiments of the activated HKUST-1 showed that pore functionalization is possible without losing the overall structural information. Added to these particularly interesting structural characteristics, HKUST-1 presents relevant magnetic properties [150]. As shown in Fig. 14, this porous coordination polymer shows a minimum in its χ versus T plot at around 70 K and an increase at lower temperatures. Fitting high-temperature data to the Curie–Weiss law gives a positive Weiss constant of 4.7 K. This magnetic behaviour can be explained by the presence of the expected strong antiferromagnetic interactions within Cu(II) dimer and weaker ferromagnetic interactions between Cu(II) dimers, which are mediated through the *meta*-substituted phenyl rings of the ligands.

Other magnetic porous solids have been prepared using the paddle-wheel Cu(II) dimer as SBUs [151–156]. For instance, Zaworotko and co-workers proposed to combine such molecular square building blocks with the 1,3-benzenedicarboxylate ligand (*m*-BDC), i.e., a V-shape spacer, to generate two porous frameworks, according to the self-assembly of two different SBUs: a triangular SBU, formed by three connected paddle-wheel Cu(II) dimers, or a square SBU, formed by four connected

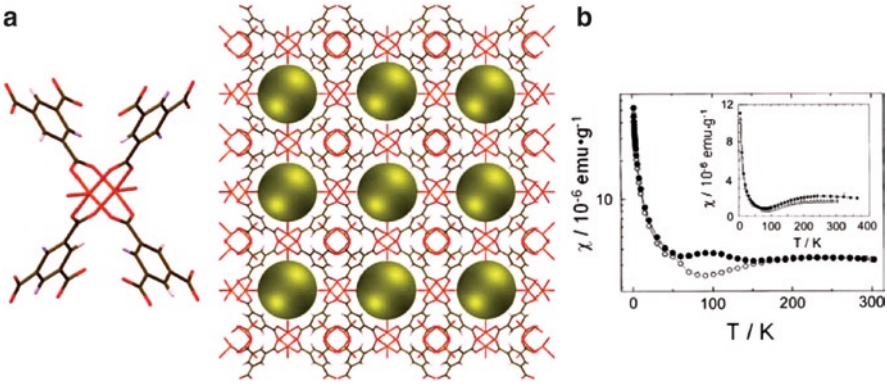

Fig. 14 (a) Paddle-wheel copper (II) tetracarboxylate building block for $[Cu_3(C_9O_6H_3)_2(H_2O)_3]$ and view of the open-framework showing nanochannels with fourfold symmetry. The empty space is represented as yellow spheres. (Cu, *orange*; O, *red*; C, *brown*; H, *white*). (**b**) Zero-field cooled (○) and field-cooled (•) temperature dependent magnetic susceptibility. Reprinted with permission from ref 150. Copyright 2000, American Institute of Physics.

paddle-wheel Cu(II) dimers. The first of such structures, $[(Cu_2(py)_2(m\text{-}BDC)_2)_3]_n$, was generated from the self-assembly of the triangular SBU to yield a Kagomé lattice with hexagonal channels presenting dimensions of 9.1 Å [151, 152]. The second structure, $[(Cu_2(py)_2(m\text{-}BDC)_2)_4]_n$, was generated from the self-assembly of Cu(II) dimers with a square topology to lead a 2-D network with channels formed by narrowed windows (1.5 × 1.5 Å) and large cavities with maximum dimensions close to 9.0 × 9.0 × 6.5 Å [153]. As for HKUST-1, the Kagomé lattice shows high rigidity in the absence of solvent guest molecules and pyridine ligands, which can be removed at a temperature of 473 K without losing crystallinity. Its most interesting feature is the report of remnant magnetization even at room temperature, due to the magnetic spin frustration associated with its triangular lattice [154], although this result seems to be controversial based upon the molecular character of this material. In contrast, the 2-D framework with a square-like arrangement of the dimeric units does not present any remnant magnetization due to lack of any geometrical frustration. In this context, its magnetic behaviour is comparable to that already observed for HKUST-1, with Cu···Cu intradimer antiferromagnetic interactions of −238 cm^{-1}, but with antiferromagnetic interdimer interactions of −85 cm^{-1}. Examples based on ligands such as 1,3,5,7-adamantane tetracarboxylate and 1,2,4,5-benzenetetracarboxylate have also been reported. In the first case, the porous coordination polymers formed present a typical inorganic platinum sulphide-based topology, a high porosity and a surface area of 560 $m^2 \cdot g^{-1}$ for their activated form [155]. For the second ligand, a 2-D coordination structure with rectangular pores of 6.0 × 7.0 Å is obtained [156]. In both solids, strong antiferromagnetic Cu···Cu intradimer antiferromagnetic interactions are observed.

Finally, channel-like magnetic frameworks built from the spacing of dimers other than the paddle-wheel dimer can also be found. To date, coordination polymers composed of nitrogen-bridge [157], oxo-bridge [156, 158], carboxylato-bridge [156, 159], and mixed oxo/carboxylato-bridge [160] dimers have been reported. For example, Liu et al. reported a family of coordination polymers formed around dicobalt(II) building blocks linked through nicotinate ligands that show robust open-framework structures up to 570 K, with antiferromagnetic coupling within the cobalt dimers [160].

4.3 Networks Based on Isolated Metal Ions and Polytopic Organic Ligands

A large variety of open-framework solids prepared using carboxylate ligands composed of a six-member ring (phenyl or a cyclohexane) backbone substituted with two or more carboxylate functional groups are known. However, even though the magnetic properties of many of them are not described, the magnetic exchange interactions between metal ions are expected to be weaker in comparison with the coordination polymers described so far in this section. For example, two complexes formed by Ni(II) macrocycles linked by BTC ligands show structures

with large channels (ca. 11 Å), but they only behave as paramagnets with very weak antiferromagnetic interactions at low temperatures [161]. Similarly, other coordination polymers prepared using benzene carboxylates with the general formula $CH_{6-n}(COO^{-})_n$ exhibit comparable weak interactions [162–164]. Besides these examples, different kinds of ligands such as N-containing or mixed N- and COOH-containing polytopic ligands have also been successfully used in the construction of porous and magnetic MOFs. This subsection provides some examples of coordination polymers obtained by this approach, or using both polytopic COOH and N-based ligands. In the last part, a strategy inspired from the "metal-radical" approach [50], which is based on the use of paramagnetic-organic polytopic open-shell ligands, is highlighted.

4.3.1 Nitrogen-Based Polytopic Ligands

Open-frameworks constructed around ditopic N-based ligands such as bipyridine have been recently reviewed. These systems show contrasting porosities, but ligands such as bipyridine usually afford solids only presenting antiferromagnetic interactions at low temperatures [5]. Examples based on tetratopic ligands such bispyrazolate, bistriazolate, or extended versions of bipyridine, among others, have also been described [165]. If these ligands do not allow an efficient transmission of magnetic interactions between isolated metal centres, porous solids showing SCO properties can be accessed [166, 167]. For example, Kepert and co-workers have reported a series of nanoporous SCO coordination polymers based on extended 4,4'-bipyridine derivatives as ditopic ligands (Fig. 15).

The complexes $[Fe_2(ligand)_4(NCS)_4]\cdot\times$ guest (guest = ethanol, acetone) consist of almost orthogonal doubly-interpenetrated 2-D (4,4) rhombic grid layers built from the linkage of Fe(II) by different ditopic ligands. In the coordination polymer

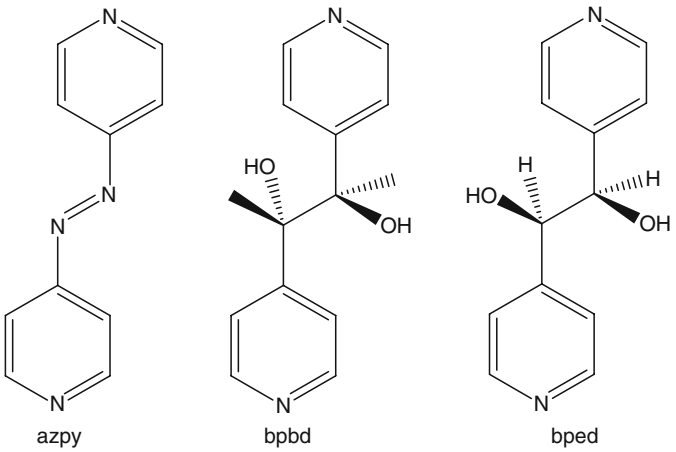

Fig. 15 Extended 4,4'-bipyridine used as ditopic ligands

of $[Fe_2(azpy)_4(NCS)_4]$·EtOH, this interpenetration leads to the formation of two kinds of 1-D channels with dimensions of 10.6 × 4.8 and 7.0 × 2.1 Å, respectively [166]. These channels run in the same direction and are filled with ethanol molecules. Loss of guest ethanol occurs at 373 K and is accompanied by several reversible structural changes. The as-synthesized sample exhibits a constant effective magnetic moment of 5.3 μB between 300 and 150 K. Below this temperature, the magnetic moment decreases, reaching a constant value of 3.65 μB due to the SCO interconversion from a fraction of the Fe(II) ions in the material. In contrast, the evacuated sample does not show SCO behaviour, but exhibits a constant magnetic moment around 5.1 μB corresponding to two crystallographic HS Fe(II) ions.

Smaller and simpler molecules such as imidazole or pyrimidinol derivatives have also been used with success to construct porous and magnetic solids. Compared to their extended analogues, they offer shorter magnetic exchange pathways that help generate stronger magnetic interactions between isolated magnetically active metal ions. For instance, Gao, You, and co-workers have reported a family of Co(II) imidazolates (im) complexes showing a variety of open-framework structures with different magnetic behaviours [168]. In this case, the rational use of solvents and counter-ligands plays a key role to obtain a collection of polymorphic 3-D porous Co(II) structures: $[Co(im)_2]$·0.5py, $[Co(im)_2]$·0.5Ch, $[Co(im)_2]_2$, $[Co(im)_2]_4$, and $[Co_5(im)_{10}$·0.4 Mb$]_5$ (py = pyridine, Ch = cyclohexanol, Mb = 3-methyl-1-butanol). Complexes $[Co(im)_2]$·0.5py and $[Co(im)_2]$·0.5Ch are isostructural, formed by Co(II) centres linked into boat- and chair-like six-membered rings connected in an infinite diamond-like net. This conformation affords 1-D channels of dimensions 5.3 × 10.4 Å and 6.6 × 8.4 Å (Fig. 16a). The crystal structure of $[Co(im)_2]_4$ shows four-membered ring Co(II) units, which are doubly-connected to wavelike or double crankshaft-like chains. These chains intersect with those running along the perpendicular axis by means of the common four-rings at the wave peaks. Three such frameworks are interwoven and linked by the imidazolates at the Co(II) ions, and the resultant 3-D framework presents 1-D helical channels of dimensions 3.5 × 3.5 Å (Fig. 16b). Similarly, the MOF $[Co(im)_2]_2$ shows identical units connected into chain units. These chains are linked by imidazolate ligands along the other two directions to give a 3-D framework with a pore openings of 4.0 × 4.0 Å (Fig. 16c). Of special structural interest is the complex $[Co_5(im)_{10}$·0.4 Mb$]_5$, which shows an open structure of zeolitic topology (Fig. 16d). In all polymorphous frameworks, the imidazolates ensure antiferromagnetic coupling between Co(II) ions. However, the uncompensated antiferromagnetic couplings arising from particular stoichiometries and topologies lead to spin-canting phenomena that are particularly sensitive to the structural characteristics. Thus, compound $[Co(im)_2]$·0.5py is an antiferromagnet with $T_N = 13.1$ K , while $[Co(im)_2]$·0.5Ch shows weak ferromagnetism below 15 K (Fig. 16e). Relatively strong ferromagnetism is observed below 11.5 K for $[Co(im)_2]_4$, with a coercive field of 1,800 Oe at 1.8 K, while the strongest ferromagnetism of the series is observed in $[Co(im)_2]_2$, which has a T_C of 15.5 K and a coercive field of 7,300 Oe at 1.8 K (Fig. 16f). The compound $[Co_5(im)_{10}$·0.4 Mb$]_5$ behaves as a hidden-canted antiferromagnet with a magnetic ordering temperature of 10.6 K.

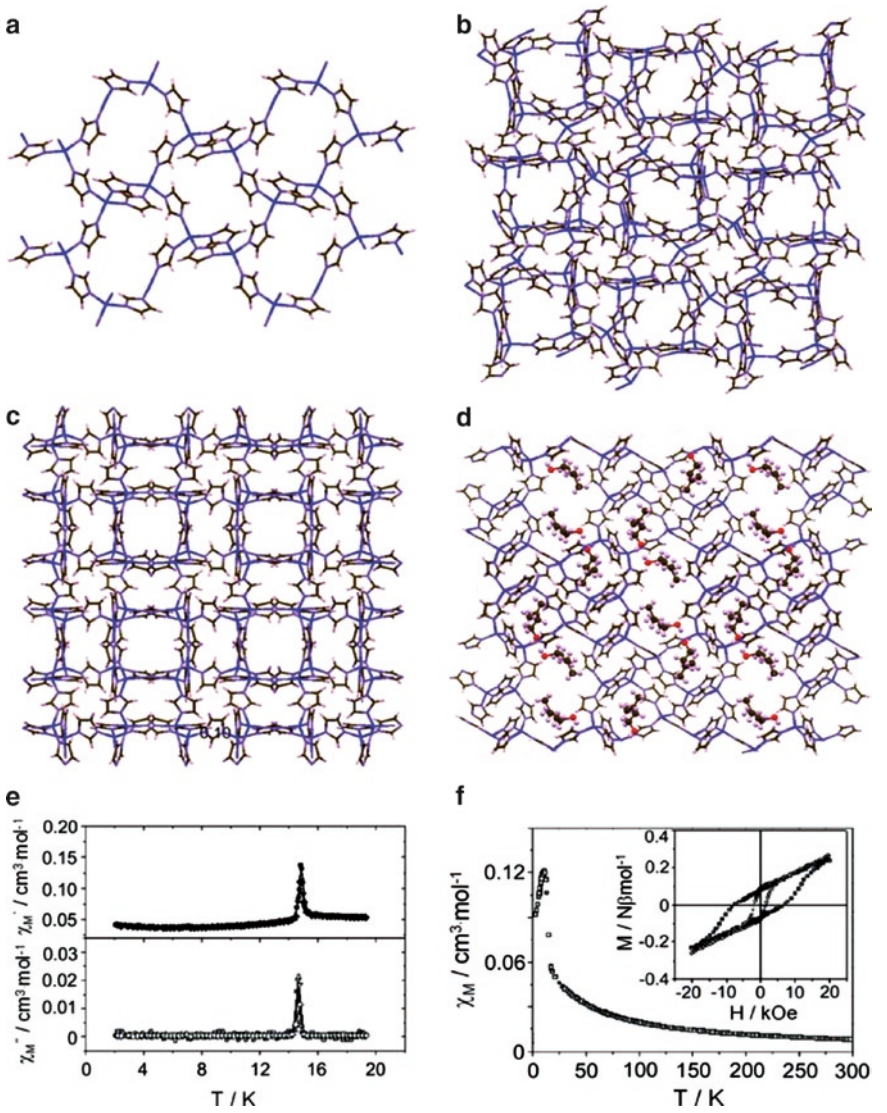

Fig. 16 Views and magnetic properties of the open-framework coordination polymers based on cobalt imidazolates. (**a**) Evacuated $[Co(im)_2]\cdot 0{\bullet}5Ch$. (**b**) $[Co(im)_2]_4$. (**c**) $[Co(im)_2]_2$. (**d**) $[Co_5(im)_{10}{\bullet}0.4Mb]_5$. (**e**) Plots of temperature dependence of ac susceptibility obtained at 0.1 Oe field for $[Co(im)_2]$ 0.5Ch. A peak appears at 15 K, which is indicative of the ferromagnetic character of this compound. (**f**) Plot of the thermal evolution of the χ_M for $[Co(im)_2]_2$ at 10 kOe field. The inset shows the hysteresis loop at 1.8 K (□) and 5.0 K (○). (Co, *blue*; O, *red*; C, *brown*; N, *violet*; H, *white*. Solvent guest molecules in (**d**) are represented as spheres) Reprinted from ref 168 [Tian YQ, Cai C-X, Ren X-M, Duan C-Y, Xu Y, Gao S, You X-Z, "The Silica-Like Extended Polymorphism of Cobalt(II) Imidazolate Three-Dimensional Frameworks: X-ray Single-Crystal Structures and Magnetic Properties" (2003) Chem Eur J 9:5673]. Copyright Wiley-VCH Verlag GmbH & Co. KGaA. Reproduced with permission

Ligands such as pyrimidin-2-ol [169] and pyrimidin-4-ol [170] have also been extensively used in this material chemistry. In 2006, Galli, Navarro, and co-workers reported a series of microporous and isomorphous coordination polymers based on 5-X-pyrimidin-2-olate ligands (referred to as 5-X-2-pymo; X = H, Cl, Br, I) [171]. All the complexes are isomorphous, with a formula $[Co(5\text{-X-2-pymo})]_n$, and show a diamondoid 3-D topology. Depending on the substituent X, important changes are observed for the magnetic properties at low temperatures. While the pyrimidinolate ligands transmit antiferromagnetic coupling between Co(II) ions, the uncompensated antiferromagnetic coupling arising from the diamondoid topology leads to magnetic ordering through spin-canting phenomena below T_N, ranging from 20 to 23 K. The spin-canting phenomena are sensitive to the ligand structure and a significant enhancement of the magnetic hardness takes place in the halo-substituted derivatives compared to the hydrogenated analogues. Thus, the coercive fields decrease in the following sequences: 2,500, 1,000, 775, and 500 Oe for X = Br, Cl, I and H, respectively, while the remnant magnetisation follows the trend 0.0501 μB for X = Br, 0.0457 μB for X = Cl, and 0.0358 μB for X = H. Interestingly, the authors also reported the preparation of molecular alloys (X = 0.5 Br + 0.5 Cl or 0.5 Br + 0.5 I), which are intermediate properties compared to the above examples.

4.3.2 Nitrogen and Carboxylic-Based Polytopic Ligands

Polymeric architectures generated by the linkage of magnetically active metal ions through mixed carboxylic and *N*-based ligands, or through ligands combining both functionalities, have also been reported [172–178].

A perfect illustration of this approach is given by the coordination polymer $\{[Co_3(IDC)_2(4,4'\text{-bpy})3]\cdot 6H_2O\cdot DMF\}_n$ reported by Cao and co-workers [175]. In this porous solid, reaction between imidazoledicarboxylic acid ($IDCH_3$) and Co(II) ions yields triangular SBUs. These SBUs exchange corners to afford a 2-D-honeycomb-like network with 24-membered metallacycles composed of six IDC^{3-} anions and six Co(II) cations. The different graphene-like layers are pillared, thanks to 4,4'-bipyridine, the nitrogen atoms completing the coordination sphere of Co(II) ions belonging to neighbouring layers.

As a result of this connectivity, hexagonal channels running parallel to the 4,4'-bipyridine are obtained (Fig. 17). These channels, which present a 12 Å diameter, are filled with water and DMF molecules. Guest solvent molecules departure is completed at a temperature of 450 K without losing the structural integrity, and both the as-synthesized and evacuated samples show weak Co···Co antiferromagnetic interactions at low temperature.

One of the most successful families is represented by a series of polymers built from the linkage of metallic carboxylate chains through 4,4'-bipyridine spacers [176]. As an example, the coordination polymer $[Cu(C_4H_4O_4)(4,4'\text{-bpy})(H_2O)_2]\cdot 2H_2O$ is formed by the connection of chains of Cu(II) metal ions bridged by succinate ligands through 4,4'-bipyridine molecules. This 3-D framework shows weak ferromagnetic interactions and channels, in which the water molecules are located.

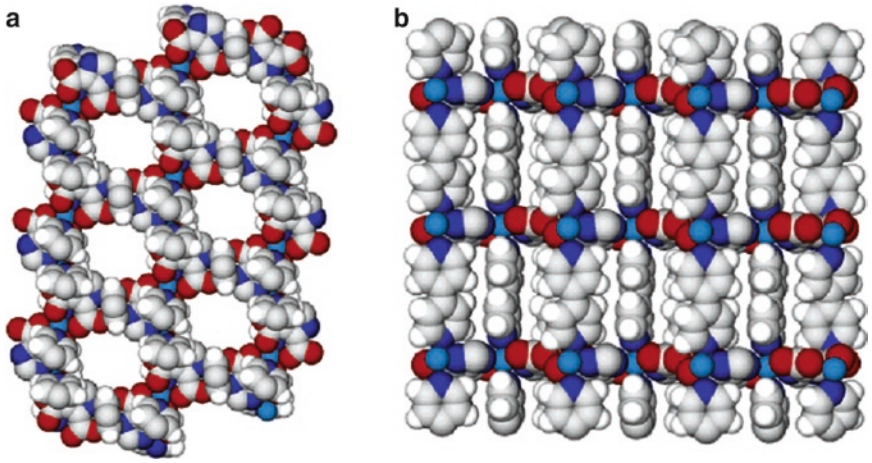

Fig. 17 Open-framework architecture of $\{[Co_3(IDC)_2(4,4'\text{-bpy})3]\cdot 6H_2O\cdot DMF\}_n$. (**a**) Top view showing the 12 Å in diameter hexagonal channels. (**b**) Side view showing the graphene-like layers pillared through bipyridine ligands (Co, *light blue*; O, *red*; N, *dark blue*; C, *grey*; H, *white*) Reprinted with permission from ref 175. Copyright 2005, American Chemical Society

Almost similar connectivity and magnetic properties are observed in the porous solid $[Fe(C_4O_4)(4,4'\text{-bpy})(H_2O)_2]\cdot 3H_2O$ [177]. Chains of Fe(II) metal ions bridged by squarate ligands are connected through 4,4'-bipyridines to form a framework with 1-D channels filled with water molecules. Interestingly, the dehydration/rehydration process in this coordination polymer, as well as in other isostructural polymers with other metal ions, is fully reversible and accompanied with a continuous change of the colour [178].

4.3.3 Organic Open-Shell Polytopic Ligands

In all the examples described so far, it can be noted that when the distance between metal ions increases, the magnetic coupling decreases. As already introduced in Section 2, magnetic coupling between metal ions generally takes place through a superexchange mechanism involving the ligands, a mechanism that is dependent on their relative orientations, and especially on the distance between magnetically active metals. Since the synthesis of larger pore sizes in coordination polymers is usually achieved by using longer organic spacers, the preparation of porous materials with increasing pore size dimensions and simultaneous long-range magnetic properties is a challenge.

The use of organic radicals as polytopic ligands is particularly attractive since these molecules are expected to act as magnetic relays between metal ions, thus allowing larger magnetic couplings and dimensionalities compared to those built from diamagnetic polytopic ligands [179]. However, the number of examples showing

high dimensionality architectures is limited due to synthetic considerations linked to ligand preparation and the coordination polymer formation [180]. In order to prepare porous and magnetic coordination polymers following this approach, the organic open-shell ligands must fulfill a series of conditions. They must have the correct geometry to induce the formation of open-framework structures, exhibit high chemical and thermal stability, and be able to interact magnetically with transition metal ions. To fulfill all three conditions, a strategy based on the use of polychlorinated triphenylmethyl tricarboxylic acid radical (PTMTC) as ligands has been developed. The conjugated base of the PTMTC radical can be considered an expanded version of the BTC ligand, where the benzene-1,3,5-trityl unit has been replaced by an sp^2 hybridized carbon atom decorated with three 4-substituted 2,3,5,6-tetrachlorophenyl rings. Therefore, PTMTC would be expected to yield open-frameworks structures similar to BTC. In addition, polychlorinated triphenylmethyl radicals have their central carbon atom, where most of the spin density is localized, sterically shielded by the encapsulation, with six bulky chlorine atoms that greatly increase their lifetime and thermal and chemical stability [181]. A family of monomeric complexes using a similar PTM radical with only one carboxylic group (PTMMC) has confirmed the feasibility of this type of carboxylic-based radicals to interact magnetically with metal ions [72, 182, 183].

Using these types of open-shell polytopic ligands, a series of metal-organic radical open-framework (MOROF-n), Fig. 18 have been prepared. Interestingly, the crystal structure of $[Cu_3(PTMTC)_2(py)_6(EtOH)_2(H_2O)]$ (MOROF-1) reveals a 2-D honeycomb (6,3) network with very large 1-D hexagonal nanopores measuring 3.1 and 2.8 nm between opposite vertices and composed of a ring of six metal units and six PTMTC radicals. The long through-space distances between the magnetic Cu(II) ions in MOROF-1 do not prevent long-range magnetic ordering. Each open-shell PTMTC ligand is able to magnetically bridge three Cu(II) ions and, therefore, extend the magnetic interactions across the infinite layers, giving a

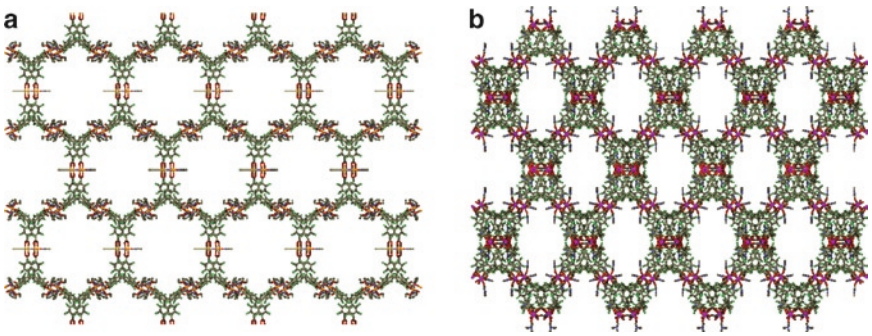

Fig. 18 Open-framework architectures for (**a**) MOROF-1 and (**b**) MOROF-4. (**a**) has been adapted from ref 63, by permission from Macmillan Publishers Ltd: Nature Materials. Copyright (2003). http://dx.doi.org/10.1038/nmat834. (**b**) has been adapted from ref 186 by permission of The Royal Society of Chemistry. http://dx.doi.org/10.1039/b802196a

ferrimagnetic layer. The solid thus shows an overall magnetic ordering at low temperatures, around 2 K [63], which is probably produced by the magnetic dipolar interactions between the large magnetic moments developed in each layer at this temperature.

Reaction of the PTMTC ligand with Co(II) ions yielded two other supramolecular Co(II)-based MOROF, namely $[Co(PTMTC)(4,4'\text{-bpy})(H_2O)_3]\cdot 6EtOH\cdot 2H_2O$ (MOROF-2) and $[Co_6(PTMTC)_4(py)_{17}(H_2O)_4(EtOH)]$ (MOROF-3). MOROF-2 presents an unprecedented $(6^3)\cdot(6^8\cdot 8^1)$ topology and exhibits helical nanochannels of dimensions 13.2 × 9.4 Å, along with antiferromagnetic interactions [184]. MOROF-3 exhibits a (6,3)-helical network with large 17.5 × 6.8 Å 1-D channels and a bulk magnetic ordering below 1.8 K [185]. More recently, the same ligand has also been reacted with magnetic Ln(III) ions to afford a series of highly porous and magnetic coordination polymers. As an example, the coordination polymer $[Tb(PTMTC)(DMF)_3]$ (MOROF-4) shows a diamond-like architecture resulting from the corner sharing of tetrahedron SBUs made by 4 PTMTC ligands and 8 Tb(III) ions. Similar to some zeolite structures such as sodalite, the connectivity of the large SBUs in MOROF-4 creates large pore sizes of dimension 22.2× 11.3 Å and generates 2-D channels running along the *a* and *b* axes. These cavities are large enough to endow this material with a total potential void volume of 61.7% of the cell volume. In this solid, PTMTC-Tb(III) ferromagnetic interactions are observed at a low temperature [186].

5 Magnetic and Porous Materials with Flexible Frameworks

One of the most remarkable characteristics of many molecule-based porous materials is their structural flexibility [187]. This feature not only concerns 0-D coordination polymers, but all the dimensionalities of the inorganic subnetworks, as well as pure organic porous materials. Thus, dynamic structural transformations such as the selective removal and resorption of solvent molecules followed by reversible crystal transformations have become one of the most intriguing properties observed for these porous materials ([188] and references cited therein). So far, two main types of dynamic structural transformations have been described. The first class deals with a reversible crystal-to-amorphous transformation that occurs when the framework collapses upon removal of guest solvent molecules and regenerates under initial or similar conditions. The second type corresponds to frameworks showing a phase transition; a crystal-to-crystal transformation. In the latter case, although removal or exchange of guest molecules results in reversible structural changes within the network, the crystalline character is maintained throughout. The structural flexibility of the coordination polymer originates from the changes in the degree of freedom (rotations, stretching, scissoring, breathing, etc.) of bonds (coordination bonds, hydrogen bonds, π–π stacking, van der Waals interactions) linking the units in the polymeric material. Thus, when a structural variation is induced by an external perturbation, for example on uptake/release of

guest molecules, a cooperative transformation of the macroscopic structure occurs, but causes no wide-range degradation of the crystal phase. An excellent account of main factors involved in such dynamic structural transformations has been published by Kitagawa et al. [40].

Recently, several authors have pointed out the possibility of using these reversible structural transformations to design a novel generation of multifunctional porous solids suitable as potential sensors. Since most of the functionalities known in porous solids are closely dependant on their crystal structure, reversible transformations upon sorption/removal of guest molecules can conveniently induce reversible modifications of the associated functionalities. This, together with the high selectivity usually shown for dynamic solids, provides the ideal scenario for researchers to create selective sensing open-frameworks for molecular recognition. Some recent examples of dynamic porous solids exhibiting tuneable magnetic properties will be presented, and a rare example of a MOF showing fascinating gas induced modulation of magnetic properties will be highlighted.

5.1 Solvent-Induced Modulation of Magnetic Properties

Kahn's group can be considered pioneer in the discovery of coordination polymers that combine both porosity and magnetism, coupled with the modulation of magnetic properties arising from guest-induced phenomena [189, 190]. In their seminal paper, published in 1999 [191], they first introduced the concept of a "molecular magnetic sponge" for a coordination polymer. As an example of these sponge-like polymers, the compound $[CoCu(obbz)(H_2O)_4]\cdot 2H_2O$, (obbz = N,N'-bis(2-carboxyphenyl)oxamido) shows a two-step reversible hydration/dehydration process followed by a dramatic change in the magnetic properties [192]. As a consequence of the first dehydration at 373 K, the discrete units link together to form a 1-D structure that behaves as a ferrimagnet with no ordering down to 2 K. A second dehydration process takes place on heating the sample up to 473 K. The resulting presumed 2-D structure still behaves as a ferrimagnet, but with a critical temperature of 30 K. All these processes are completely reversible, and the material can be rehydrated after cooling with the recovering of the initial magnetic properties.

Several examples of porous and magnetic coordination polymers showing solvatomagnetic effects have been reported. In 2003, the open-framework coordination polymer $[Cu_3(PTMTC)_2(py)_6(EtOH)_2(H_2O)]$ (MOROF-1; see also Section 4.3.3), which combines very large pores (3.1 × 2.8 nm, and a 65% void volume) with magnetic ordering around 2 K, was reported [63]. Added to these properties, another particularly interesting feature was observed for this material: the reversible "shrinking-breathing" process observed on solvent uptake and release, which, in turn, induces changes in magnetic properties (Fig. 19a).

On removal from solution and exposed to air, crystalline MOROF-1 loses guest solvent molecules very rapidly, becoming an amorphous magnet with a lower critical temperature (Fig. 19b). The critical temperature is determined not only by the

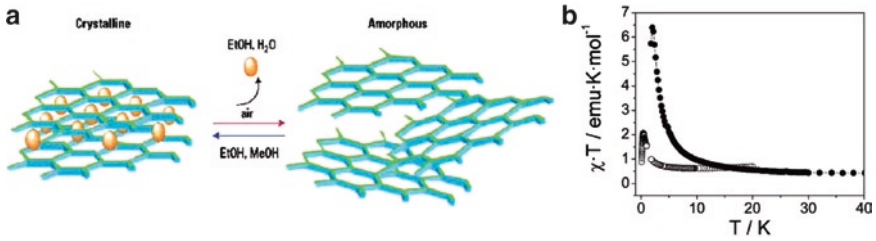

Fig. 19 (**a**) Schematic representation of the reversible crystal-to-amorphous transformations in MOROF-1. Reprinted from ref 193, by permission from Macmillan Publishers Ltd: Nature Materials. Copyright 2003. http://dx.doi.org/10.1038/nmat837. (**b**) Plot of χ_M·T versus temperature for as-synthesized (•) and evacuated (○) MOROF-1. The graph has been adapted from ref 63

strength of the magnetic interactions between the spins but also by the dimensionality of such interactions and hence, the crystal packing of the network. However, the evacuated sample of MOROF-1 experiences a transformation, recovering its original crystallinity and magnetic properties after exposure to ethanol solvent. Unexpectedly, this behaviour is only observed when MOROF-1 is exposed to small alcohols like methanol and ethanol, showing a large selectivity for these two molecules among 16 larger alcohols assayed [63]. Contrasted solvatomagnetic effects have been described in several molecular porous materials reported by Kurmoo and co-workers. For example, reversible dehydration/rehydration processes in the porous and magnetic solids $[Co_3(OH)_2(\mathbf{2})_2]\cdot 3H_2O$ and $[Ni_3(OH)_2(C_8O_2H_{10})_2(H_2O)_4]\cdot 2H_2O$ induces reversible transformations from ferromagnetic to antiferromagnetic ordering and from ferromagnetic to ferrimagnetic ordering, respectively (Fig. 20b) [194, 195].

In contrast to the large structural transformations experienced by MOROF-1, where volume variations close to 30% are observed between the as-synthesized and the amorphous guest-free solid, these latter interconversions are accompanied by subtle changes in crystal structure. For example, the dehydration process in $[Co_3(OH)_2(\mathbf{2})_2]\cdot 3H_2O$ only involves minimum changes in its structure, with almost no change in the coordination environment of the metal ions (Fig. 20a). This fact clearly suggests that the ferromagnetic ground state in the hydrated phase may be caused by the presence of significant magnetic exchange coupling through the hydrogen bonded water molecules located within the channels.

The influence of sorbed guest molecules on magnetic properties was also nicely evidenced in the diamondoid coordination polymer $[Mn_3(\mathbf{1})_6]\cdot CH_3OH\cdot H_2O$, in which the magnetic ordering temperature depends on the guest molecules in the framework (very recently, guest influence on magnetic properties in a series of isomorphous compounds of formula $[Fe_3(\mathbf{1})_6]\cdot$x guest (with x = iodine, THF, furan, benzene, acetonitrile, and acetone) has also been explored in detail [196]). Indeed, magnetic measurements of the as-synthesized or evacuated sample show a long-range magnetic ordering with a critical temperature close to 8 K. However, this critical temperature can be modulated from 5 to 10 K by the sorption of several

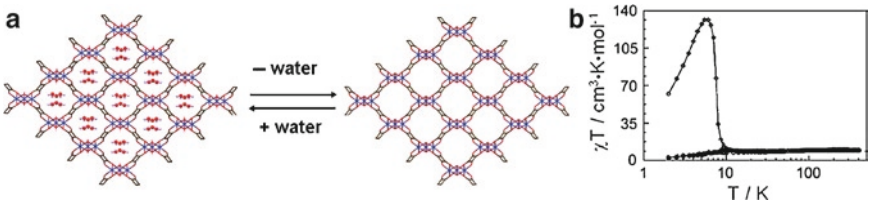

Fig. 20 Structure and magnetic properties in $[Co_3(OH)_2(\mathbf{2})_2]\cdot 3H_2O$ (**a**) Almost similar as synthesized and evacuated solids (water molecules are represented as spheres). (**b**) Strong modulation of the magnetic properties between as-synthesized (○) and evacuated (•) materials. Reproduced from ref 43 by permission of The Royal Society of Chemistry. http://dx.doi.org/10.1039/b501600m

types of guest molecules. This transformation can be explained by the small changes of the Mn–O–Mn bond angles – the larger the angle, the smaller the T_C – which are modulated on absorption of guest molecules. Very recently, the same authors have also shown this framework to become optically active when enantiomerically pure 2-chloropropan-1-ol molecules are inserted in its channels [197]. The apohost framework is achiral but incorporates channels of opposite handedness (+) *P* and (−) *M*. Upon insertion of either *R* or *S* chiral solvent molecules the two corresponding chiral solids – *R* and *S*, respectively, are obtained. These results are explained by the fact that in the obtained chiral *R* framework the *R* molecules better match the *M* channels and are disordered in the *P* channels, while in the *S* framework the *S* molecules are ordered in the *P* channels and disordered in the *M* channels. In contrast, with the addition of a racemic solvent mixture, the meso compound can be obtained. In this case, random disorder of the two guests in both kinds of channels is observed. All the solids resulting from these loading experiments show a ferrimagnetic ground state. Nevertheless, compared to the host framework, the Curie temperature decreases to 7.6 K for both *R* and *S* solids, while it slightly increases to 8.3 K in the *meso* form. In the chiral solids, additional interactions between the framework and ordered guest solvent molecules through hydrogen bonds or other electrostatic forces are responsible for the decrease in magnetic ordering temperature.

Porous solids such as Prussian Blue analogues [198, 199], in which CN^- spacers connect magnetic metal ions in the three directions, deserve to be commented upon since they could exhibit important changes in their magnetic properties and colors upon dehydratation/rehydration processes [200–202]. For example, Ohkoshi, Hashimoto, and co-workers have recently reported $Co[Cr(CN)_6]_{2/3}\cdot zH_2O$, a pink ferromagnetically-coupled magnet with a T_C of 28 K that reversibly transforms into a blue antiferromagnetically-coupled magnet with a T_C of 22 K on dehydration [203]. Such solvatomagnetism and solvatochromism are ascribed to the adsorption and desorption of ligand water molecules at the Co(II) centres. Such processes change the coordination geometry at Co(II) from six-coordinate pseudo-octahedral to four-coordinate pseudo-tetrahedral coordination, thus modulating the magnetic

interactions from ferromagnetic coupling in the hydrated solid to antiferromagnetic ones in the apohost.

Very recently, Sutter and co-workers reported a series of nanoporous and chiral magnets showing switchable ordering temperatures driven through similar H_2O sorption/desorption phenomena [204]. These coordination polymers $[\{Mn(HL)(H_2O)\}_2Mn\text{-}\{Mo(CN)_7\}_2\cdot 2H_2O$ are formed from the reaction of $\{Mo(CN)_7\}^{4-}$ with Mn(II) ions and enantiomerically pure *R*, *S* or racemic mixture of N,N-dimethylaminol (L), which acts as an ancillary ligand and confers to those materials chiral characteristics. Overall, the different structures show a 3-D cyano bridged Mn–Mo network, which has small channels running along the *c*-direction (Fig. 21a). These channels are filled with water molecules and they are defined by "Mn_4-Mo_4" rings with each $\{Mo(CN)_7\}^{4-}$ unit connecting two different Mn(II) ions. One Mn(II) ion shows a distorted tetrahedral environment consisting of four NC–Mo linkages, while the other has a distorted octahedral coordination sphere with four NC-Mo linkages and two O-atoms, one coming from the L molecule, and the other from an ancillary water molecule. Lattice and coordinated water molecules are readily removed upon heating to afford an apohost crystalline material via a phase transition.

Interestingly, the starting hydrated compound is fully recovered after the exposure of the desolvated phase to air over 50 min. As observed in the previous examples, loss of coordinated water leads to a strong modification of the coordination sphere of one of the Mn(II) ions, which changes from a distorted octahedral environment to five coordinate. This reduced coordination number leads to the shortening of the Mn-NC bonds and gives stronger Mn-Mo interactions within the framework. The hydrated material shows magnetic ordering below $T_C = 85$ K (Fig. 21b), and the ordering temperature is shifted to $T_C = 106$ K in the apohost (Fig. 21c). Since the crystal-to-crystal transformations are fully reversible, magnetic features are recovered when the framework is rehydrated.

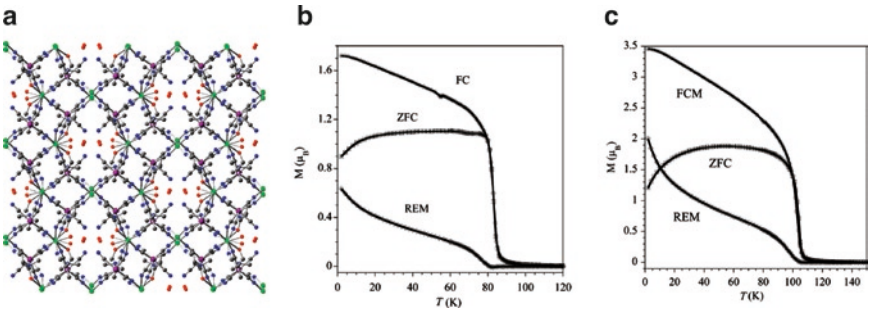

Fig. 21 (**a**) Open-framework architecture of S-$[\{Mn(HL)(H_2O)\}_2Mn\text{-}\{Mo(CN)_7\}_2\cdot 2H_2O$ (water molecules are represented as red spheres). Field cooled magnetization (○, $H = 100$ Oe), zero field cooled (□), and remnant magnetization (◊) as a function of temperature for the hydrated (**b**) and dehydrated (**c**) solids. Reprinted with permission from ref 204. Copyright 2007, American Chemical Society

5.2 Solvent-Induced Modulation of Spin-States

The influence of guest solvent molecules on SCO phenomena has been observed in flexible coordination polymers, and this functionality has been incorporated in dynamic porous solids. SCO is a cooperative phenomenon, where a given metal ion can change its spin state, from HS to LS upon exposure to an external perturbation such as change in temperature, pressure, or light. Structural modifications and both intra-framework and host–guest hydrogen bonding interactions will greatly influence the SCO interconversion in such types of solids.

Kepert and co-workers have reported a series of porous coordination polymers by the reaction of Fe(II) salts with N-based ditopic ligands [166, 205, 206]. Overall, these coordination polymers present comparable 3-D structures resulting from the interpenetration of (4,4)-rhombic grids obtained through the connection of the Fe (II) ions with the ditopic ligands (Fig. 22a). To explain the change occurring in the SCO phenomena in dynamic structures, the coordination polymer $[Fe(bpbd)_2(NCS)_2]\cdot\{Acetone\}$ can be regarded as a reference. In this solid, grid interpenetration is realized at an angle of 90° and generates 1-D channels of dimensions 14.5 × 14.5 Å, which are run along the *c*-axis. This 3-D framework is further stabilized by strong hydrogen bonds involving the diol groups of the bpbd ligand and the sulphur-donor of thiocyanate groups complete the coordination sphere of each Fe(II) ions. Noteworthy is the fact that the acetone molecules filling the channels do not participate in any short hydrogen bonding with the ligands. Consequently, guest departure is completed at 102°C and structural analysis of the apohost reveals minimal changes in the framework atoms structuring the solvated and the desolvated forms (Fig. 22b). Thus, SCO behaviour is only slightly affected by loss of solvent: while the solvated form shows a relatively abrupt one-step full spin transition with $T_{1/2} = 162$ K upon cooling, a slightly shifted similar transition ($T_{1/2} = 156$ K) is observed in the evacuated solid. As expected, both forms show comparable structure contraction, ca. 4% of the unit cell, upon cooling, which is consistent with a full spin transition [205].

Completely different behaviours are observed in the coordination polymers constructed from azpy and bped ligands (Fig. 23), in which guest ethanol molecules

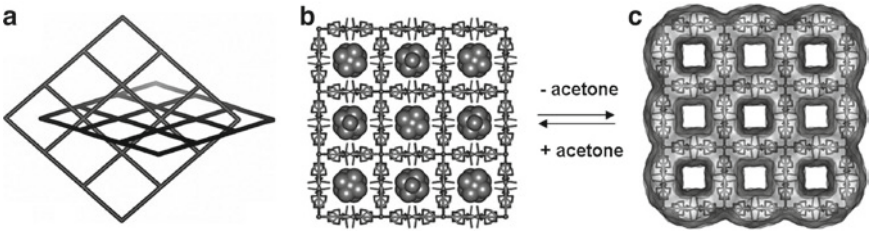

Fig. 22 (**a**) Topological representation of the orthogonal interpenetration of (4,4)-rhombic grids in the series of coordination polymers showing SCO properties. (**b** and **c**) Structure representations for $[Fe(bpbd)_2(NCS)_2]\cdot\{acetone\}$ and $[Fe(bpbd)_2(NCS)_2]$. Reproduced with permission of ref 205 [Neville SM, Moubaraki B, Murray KS, Kepert CJ "A Thermal Spin Transition in a Nanoporous Iron(II) Coordination Framework Material" (2007) Angew Chem Int Ed 46:2059]. Copyright Wiley-VCH Verlag GmbH & Co. KGaA

interact with the host framework through hydrogen bonds. The coordination polymer $[Fe_2(azpy)_4(NCS)_4]\cdot EtOH$ presents two kinds of 1-D channels with dimensions of 10.6 × 4.8 and 7.0 × 2.1 Å, respectively. These channels are filled with ethanol molecules, which interact through hydrogen bonds with the sulphur centres of the thiocyanate ligands bound to Fe(II) ions. As a consequence, guest loss upon heating leads to important structural changes in the apohost. The most significant change is an elongation and constriction of the 1-D channels to new dimensions of 11.7 × 2.0 Å. This structural modification induces enormous changes in the electronic behaviour of this compound. While the as-synthesized sample exhibits a broad half SCO transition at 150 K, the evacuated one shows a constant magnetic moment of 5.1 μB, lacking any SCO transition. Surprisingly, the original SCO properties are recovered after resorption of the guest solvent molecules, this phenomena being also observed with small alcohols such as methanol or propanol (Fig 23a) [166].

Grid interpenetration at an angle of 85.2° is observed in the coordination polymer $[Fe(bped)_2(NCS)_2]\cdot 3EtOH$, which incorporates channels of dimensions 8.4 × 4.7 Å separated by narrower polar windows of dimensions 6.4 × 6.3 Å. Channels and windows are filled with ethanol molecules that interact through hydrogen bonds with OH-groups of the bped ligands, which are also involved in intra-framework interactions through strong hydrogen bonds with the sulphur centres of thiocyanate ligands. The most important structural change upon guest removal is an increase in the interpenetration angle from 85.2° to 90°. Consequently, the accessible void volume changes from 31.0 to 34.9%, and is associated with a dilatation of the cavities and a contraction of the polar windows. Loss of guest molecules leads to new intra-framework interactions, which tend to stabilize the apohost. As in the previous case, these structural modifications are of paramount importance to the SCO interconversion. While the starting material shows a broad and uncompleted SCO interconversion at $T_{1/2} = 137$ K, the $T_{1/2}$ decreases to ca. 125 K in the aphohost with a transition over a wider temperature range (225–270 K) (Fig 23b). Additionally, the fraction of residual HS Fe(II) is as well higher: ca. 53% in the solvated material compared to 37% in the solvated solid [206].

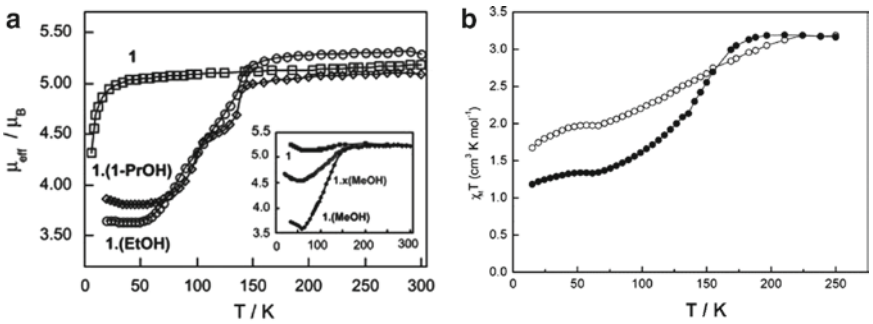

Fig. 23 (**a**) Temperature-dependent magnetic moment of $[Fe_2(azpy)_4(NCS)_4]\cdot x(guest)$, (**1·x**(guest) in the scheme). The inset shows the effect of partial and complete removal of Methanol from **1**·methanol. Reprinted from ref. 166 with permission from AAAS. (**b**) Plot of $\chi_M \cdot T$ versus temperature for $[Fe(bped)_2(NCS)_2]\cdot 3EtOH$ (•) and the corresponding apohost (○) Reprinted with permission from ref 206. Copyright 2008, American Chemical Society

Very recently, a molecule-based nanoporous coordination polymer showing tuneable SCO behaviour near room temperature has also been reported by Aromí, Gamez, and co-workers [207]. In this case, reaction of the $[Fe_2(dpya\text{-}triz)_2(CH_3CN)_2(H_2O)_2]^{4+}$ ditopic SBUs with Fe(II) affords a purple 1-D coordination polymer $\{[Fe_3(dpya\text{-}triz)_2(CH_3CH_2CN)_4(BF_4)_2](BF_4)_4{\cdot}4(CH_3CH_2CN)\}_n$ (dpya-triz = 2,4,6-tris-(di(pyridin-2-yl)amino)-1,3,5-triazine. Overall, packing of 1-D chains results in the formation of channel-like cavities with a cross section of ca. 6 × 4 Å, in which reside lattice solvent molecules and non-coordinated tetrafluoroborate anions. Interestingly, this coordination polymer shows a HS to LS SCO process at ca. 300 K involving 2/3 of the Fe(II) centres. Upon guest removal, a crystal-to-crystal transformation occurs with all the guest and coordinated propionitrile molecules being exchanged with water molecules. The solid turns to yellow and the SCO transition is lost. Interestingly, this phenomenon is fully reversible and both the starting structure and properties are recovered upon immersion in propionitrile or acetonitrile. With the latter solvent, the SCO transition is shifted to lower temperatures ($T_{1/2} = 275$ K).

Similar reversible properties have been found in another compound reported by Real, Bousseksou, and co-workers [208, 209]. $[Fe(pmd)(H_2O)\{Au(CN)_2\}_2]{\cdot}H_2O$ (pmd = pyrimidine) shows a triply interpenetrated structure and a sharp half SCO transition at 165 K with a hysteresis of approximately 8 K. The dehydration process induces large changes in the crystal structure with the pyrimidine ligands, previously bound only through one nitrogen atom, now bridging two Fe(II) ions. This results in the linkage of the three independent interpenetrated frameworks into a unique 3-D network. This conversion results in the suppression of the SCO behaviour, which can be recovered on rehydration. Interestingly, the isostructural $[Fe(pmd)(H_2O)\{Ag(CN)_2\}_2]{\cdot}H_2O$ shows a similar reversible behaviour, but with a shift of the SCO transition to lower temperatures for the dehydrated phase.

5.3 Gas-Induced Magnetic Properties Modulation

Although the number of examples of solvent-induced magnetic properties or spin-state modulation is increasing, cases of coordination polymers in which magnetic properties are modulated upon gas adsorption are rare. While several organometallic compounds containing CO_2 are known [210, 211], the first example of magnetic framework trapping CO_2 during its synthesis was reported by Cornia and co-workers in 1999 [83]. Nevertheless, magnetic properties of the activated framework and eventual reversible trapping were not reported.

The ultramicroporous 3-D MOF $[Cu(F\text{-}pymo)_2(H_2O)_{1.25}]_n$ (F-pymo = 5-fluoropyrimidin-2-olate) reported by Navarro, Parra, Sironi, and co-workers [212] displays a zeolitic gismondine-like topology with helical channels of ca. 2.9 Å diameter. These channels result from the interconnection of two different cyclic motifs, namely metallacalix[8]arenes and metallacalix[4]arenes exhibiting either 1,3-alternate or a pinched cone conformation (Fig. 24a). These are filled with water

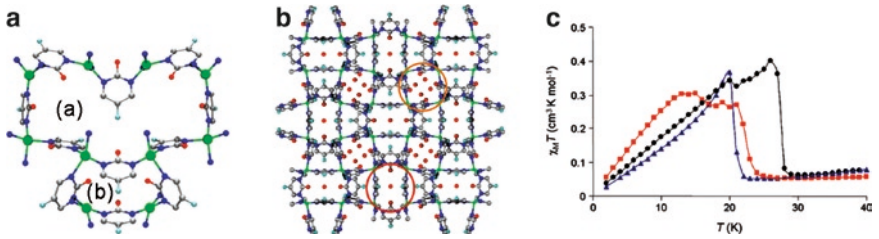

Fig. 24 Structure and magnetic properties for $[Cu(F\text{-}pymo)_2(H_2O)_{1.25}]_n$ (**a**) Metallacalix[8]arenes (**a**) and metallacalix[4]arenes (**b**) cyclic motifs. (**b**) Gismondine-like framework (guest water molecules are represented as red spheres). (**c**) $\chi_M \cdot T$ versus temperature for as-synthesized (*blue*), activated (*red*) and CO_2-loaded (*black*) materials. Reprinted with permission from ref 212. Copyright 2008, American Chemical Society

molecules, which are associated with the framework through strong hydrogen bonds (Fig. 24b). The framework remains crystalline up to 513 K after guest water removal and has a relatively small volume (ca. 13%) available for guest inclusion. At 77 K, the activated solid behaves as a molecular sieve, selectively adsorbing H_2 over N_2, possibly due to size exclusion. The case of CO_2 is even more interesting since these larger molecules are readily incorporated at temperatures as high as 433 K through a transient phase and channels expansion.

Interestingly, the authors have investigated the influence of guest molecules on the magnetic properties in this material (Fig. 24c). The as-synthesized solid shows antiferromagnetic interactions and a weak ferromagnetic ordering below $T_N = 24$ K, which arises from a spin-canting phenomenon related to the non-centrosymetric nature of the framework. While the magnetic ordering temperature is only slightly decreased in the activated material ($T_N = 22$ K), loading with CO_2 has a profound effect on the magnetic properties, since the ordering temperature is increased to 29 K. To explain this result, the authors presume that the structural perturbation exerted by the CO_2 guests may lead to a less distorted environment for the Cu(II) ions with a concomitant increase in overlap between the ligand orbitals and the metal ion magnetic orbitals, thus permitting more efficient magnetic exchange within the framework.

6 Conclusions and Perspectives

As highlighted in the previous sections, many magnetic and porous molecule-based materials with well-defined geometries have been prepared using metal ions and closed-shell and open-shell polytopic organic ligands. Due to the wide availability of organic ligands that can be combined with metal ions, a huge variety of structures is available, the properties of which can be studied for different applications similar to those developed with non-magnetic MOFs in area of catalysis [24–26], gas storage [27–35], and others [36–39]. Nevertheless, new fields of application can be envisioned by exploring the anchoring of these materials onto solid surfaces, or their processability for applications in nanotechnology and in biomedicine.

6.1 Porous and Magnetic Coordination Polymers on Surfaces

In the previous sections, we have reported examples of magnetic and porous coordination polymers. Nevertheless, it is of the utmost importance to harness the properties of such materials in solid-state applications or devices. Therefore, much effort must be devoted to the development of new methods for preparing thin films containing these multifunctional coordination polymers with the aim of directing and controlling the growth of MOFs on surfaces, and to integrate them as novel functional units for bottom-up nanotechnology [213]. The robustness of some porous coordination polymers can be exploited for loading with organometallic precursors of solids that can be subsequently converted into nanosized metal clusters or wires inside the pores [214].

Surface anchoring is a key step, crucial for applications such as the manufacturing of sensor devices. It has been recently shown that the sequential addition of molecular-sized layers to form complex structures is a way of building coordination polymers as well as other heterogeneous nanostructures on surfaces [215, 216]. This approach, named layer-by-layer, allows the building of supramolecular structures from surfaces through the self-assembly of successive monolayers of organic molecules and metal ions interacting via coordination bonds [217]. Therefore, the well-known coordination chemistry of a metal ion in solution might be used to form and control thin film structure and properties at the molecular level.

An example of this approach is represented by the growth of 3-D coordination polymers with SCO properties via stepwise adsorption reactions for multilayer films based entirely on intra- and interlayer coordination bonds Fe(pyrazine)$[Pt(CN)_4]$ [218, 219]. Indeed, after functionalization of the surface with the appropriate anchoring layer the coordination polymer is built in a stepwise fashion, alternating the metal ion (Fe^{2+}), the platinum salt ($[Pt(CN)_4]^{2-}$), and pyrazine. The polymer shows many interesting properties, with the SCO transition accompanied by a variation in the dielectric constant of the material accompanied by a room temperature hysteresis of the dielectric constants. This dielectric hysteretic property may be useful in building molecular memory devices that can store information by high- and low-capacitance states. What must be remarked here is that these appealing properties cannot be exploited in bulk materials, but only in thin films.

The approach of anchoring metal-PTM based frameworks onto solid surfaces has also been undertaken in order to graft porous and magnetic frameworks onto solid supports. So far, the feasibility of the layer-by-layer methodology has been exemplified by the monocarboxylic PTM derivative (PTMMC), the Cu(II) complex of which was successfully grafted onto a carboxylate-functionalized gold surface with its magnetic character remaining intact. Further studies on di- and tri-carboxy substituted PTM radicals coordinated to metal ions are in progress, towards the grafting of a porous multidimensional magnetic structure onto a metal surface [220].

6.2 Porous and Magnetic Coordination Cages

Use of metal-directed self-assembly has afforded many different 0-D discrete structures with internal void space, with the geometry of the organic linker dictating the observed geometry of the material [221, 222]. A variety of structures that include molecular nanosized squares and rectangles [221–223], trigonal [224, 225] and square prismatic capsules [226], as well as tetrahedral [227], octahedral, and higher order suprastructures [228, 229] have been reported. These supramolecular organizations have potential applications as chemical sensors and reaction nanovessels [223, 230–233]. It is only very recently that the first two examples dealing with the preparation of magnetic and porous cages based on open-shell radical ligands and metal subunits have been reported [234, 235]. These studies demonstrated the possibility of incorporating multidimensional metal-organic cages bearing specific functionality with predesigned physico-chemical properties. They also opened the way towards exciting potential applications; since these spin cages are soluble in water their use as new spin probes and as magnetic resonance imaging (MRI) contrast agents could be envisioned.

6.3 Porous and Magnetic Coordination Polymers as Sensors

One of the aims of recent research on coordination polymers is the design of materials combining a set of properties for specific applications. As an example, Corma, Rocha, and co-workers recently reported the rational design and preparation of lanthanide-based porous MOFs showing sensing properties [236]. Their aim was the preparation of rare-earth based MOFs showing hydrophobicity, high adsorption capacity, high thermal resistance, anisotropic photoluminescence, and magnetic properties. The authors succeeded in the preparation of such a MOF by combining an organic aromatic and hydrophobic spacer with lanthanide ions. The change in the fluorescence signal intensity is the result of the interaction of the host with ethanol in the presence of water under ambient conditions. Hence, this lanthanide-based MOF is an example of a rationally-designed sensor based on coordination chemistry.

6.4 Processability of Magnetic Coordination Polymers

Hybrid materials based on gadolinium ions have been investigated as MRI contrasting agents. However, many of these agents show toxicity that prevents their use. One of the approaches to reduce the toxicity of contrast agent is based upon the use of viral capsides as nanocontainers for gadolinium ions bound to the interior of the capside via coordination bonds; i.e., in the form of MOFs [237]. A second approach consists of the reduction of the dose of the drug given to the patient by increasing

the availability of the administrated contrasting agent. So far, good results have been reported by processing MOF-contrasting agent as soluble nanoparticles [238]. Nanoparticles might not only be of use in biomedicine, but also in nanotechnology. Their applications may range among data storage, catalysis, photonics, electronics, microlenses, and biosensors. The principal challenge is in the preparation of nanoparticles showing specific properties, i.e., nanoscale metal-organic particles. Recently, the successful preparation of nanoparticles of Prussian Blue analogues [239], or systems showing magnetic behaviours such as superparamagnetism [240], valence tautomerism [241], SMM behaviour [242] or SCO phenomena [243, 244] has been reported. It is reasonable to think that examples of porous and functional nanoparticles will follow soon [245].

Aknowledgements Authors want to thank the financial support given by the "Plan Nacional de Investigación Científica y Desarrollo e Innovación Tecnológica," Iniciativa Ingenio 2010, Programa Consolider, under Project EMOCIONA (CTQ 2006-06333/BQU), the "Instituto de Salud Carlos III" through "Acciones CIBER," the Generalitat de Catalunya (Project 2009 SGR 516), and the European Commission under the Network of Excellence "MAGMANet" (contract NMP3-CT-2005-515767-2) and the Collaborative Project "SURMOF" (contract STRP032109). V.M. thanks the Spanish Research Council (CSIC) for funding and the Spanish MICINN for a Juan de la Cierva contract.

References

1. Wilson ST, Lok BM, Messina CA, Cannan TR, Flanigen EM (1982) J Am Chem Soc 104:1146
2. Cheetham A, Férey G, Loiseau T (1999) Angew Chem Int Ed 38:3268
3. Natarajan S, Mandal S (2008) Angew Chem Int Ed 47:2
4. Férey G (2008) Chem Soc Rev 37:191
5. Janiak C (2003) Dalton Trans 2781
6. Férey G (2001) Chem Mater 13:3084
7. Cheetham A, Rao CNR, Feller RK (2006) Chem Commun 4780
8. Yaghi OM, O'Keefe M, Ocwig NW, Chae HK, Eddaoudi M, Kim J (2003) Nature 423:705
9. Moulton B, Zaworotko MJ (2001) Chem Rev 101:1629
10. Eddaoudi M, Moler DB, Li HL, Chen BL, Reineke TM, O'Keeffe M, Yaghi OM (2001) Acc Chem Res 34:319
11. Robson R (2000) J Chem Soc, Dalton Trans 37:3537
12. Zaworotko M (2000) Angew Chem Int Ed 39:3052
13. Yaghi OM, Li HL, Davis C, Richardson D, Groy TL (1998) Acc Chem Res 31:474
14. Blake AJ, Champness NR, Hubberstey P, Li WS, Withersby MA, Schröder M (1999) Coord Chem Rev 183:117
15. Rao NR, Natarajan S, Vaighyanathan R (2004) Angew Chem Int Ed 43:1466
16. Park YK, Choi SB, Kim H, Kim K, Won B-H, Choi K, Choi J-S, Ahn W-S, Won N, Kim S, Jung DH, Choi S-H, Kim G-H, Cha S-S, Jhon YH, Yang JK, Kim J (2007) Angew Chem Int Ed 46:8230
17. Park K-M, Iwamoto T (1992) J Chem Soc, Chem Commun 72
18. Kim J, Whang D, Lee JI, Kim K (1993) J Chem Soc, Chem Commun 1400
19. Yaghi OM, Li H (1995) J Am Chem Soc 117:10401
20. Yaghi OM, Li H (1996) J Am Chem Soc 118:295
21. Min KS, Suh MP (2000) J Am Chem Soc 122:6834
22. Kamiyama A, Noguchi T, Kajiwara T, Ito T (2000) Angew Chem Int Ed 39:3130

23. Uemura K, Kitagawa S, Kondo M, Fukui K, Kitaura R, Chang H-C, Mizutani T (2002) Chem Eur J 8:3586
24. Corma A (1995) Chem Rev 95:559
25. Fujita M, Kwon YJ, Washizu S, Ogura K (1994) J Am Chem Soc 116:1151
26. Sawaki T, Aoyama Y (1999) J Am Chem Soc 121:4793
27. Rosi NL, Eckert J, Eddaoudi M, Vodak DT, Kim J, O'Keefe M, Yaghi OM (2003) Science 300:1127
28. Van Den Berg AWC, Otero Areá C (2008) Chem Commun 668
29. Morris RE, Wheatley PS (2008) Angew Chem Int Ed. 47:4966
30. Férey G, Mellot-Draznieks C, Serre C, Millange F, Dutour J, Surblé S, Margiolaki I (2005) Science 309:2040
31. Eddaoudi M, Kim J, Rosi N, Vodak D, Wachter J, O'Keeffe M, Yaghi OM (2002) Science 295:469
32. Li H, Eddaoudi M, O'Keeffe M, Yaghi OM (1999) Nature 402:276
33. Kondo M, Yoshitomi T, Seki K, Matsuzaka H, Kitagawa S (1997) Angew Chem Int Ed 36:1725
34. Kondo M, Okubo T, Asami A, Noro S-I, Yoshitomi T, Kitagawa S, Ishii T, Matsuzaka H, Seki K (1999) Angew Chem Int Ed 38:140
35. Noro S-I, Kitagawa S, Kondo M, Seki K (2000) Angew Chem Int Ed 39:2081
36. Kuznicki SM, Bell BA, Nair S, Hillhouse HW, Jacubinas RM, Braunbarth CM, Toby BH, Tsapatsis M (2001) Nature 412:720
37. Pan L, Adams KM, Hernandez HE, Wang X, Zheng C, Hattori Y, Kaneko K (2003) J Am Chem Soc 125:3062
38. Dybtsev CN, Chun H, Yoon SH, Kim D, Kim K (2004) J Am Chem Soc 126:32
39. Mueller U, Schubert M, Teich F, Puetter H, Schierle-Arndt PK (2006) J Mater Chem 16:626
40. Kitagawa S, Kitaura R, Noro S-J (2004) Angew Chem Int Ed 43:2334
41. Champness NR (2006) Dalton Trans 877
42. Kepert C (2006) Chem Commun 695
43. Maspoch D, Ruiz-Molina D, Veciana J (2007) Chem Soc Rev 36:770
44. Miller JS (2000) Inorg Chem 39:4392
45. Kahn O (2000) Acc Chem Res 33(10):647
46. Buschow KHJ, De Boer R (2003) Physics of Magnetism and Magnetic Materials. Kluwer/Plenum, New York
47. Miller JS, Epstein AJ (2000) MRS Bull 21
48. Maspoch D, Domingo N, Roques N, Wurst K, Tejada J, Rovira C, Ruiz-Molina D, Veciana J (2007) Chem Eur J 13:8153
49. Roques N, Maspoch D, Datcu A, Wurst K, Ruiz-Molina D, Rovira C, Veciana J (2007) Polyhedron 26:1934
50. Caneschi A, Gatteschi D, Sessoli R, Rey P (1989) Acc Chem Res 22:392
51. Lacroix PG (2001) Chem Mat 13:3495
52. Blundell SJ, Pratt FL (2004) J Phys Condens Matter 16:R771
53. Amabilino DB, Veciana J (2001) In: Miller JS, Drillon M (eds) Magnetism: molecules to materials II. Wiley, Weinheim
54. Kahn O (ed) (1996) Magnetism: a supramolecular function. Kluwer, Dordrect
55. Amabilino DB, Cirujeda J, Veciana J (1999) Phil Trans R Soc Lond A 357:2873
56. Cirujeda J, Hernàndez-Gasió E, Rovira C, Stanger J-L, Turek P, Veciana J (1995) J Mater Chem 5(2):243
57. Deumal M, Cirujeda J, Veciana J, Novoa JJ (1998) Adv Mater 10(17):1461
58. Kinoshita M, Turek P, Tamura M, Nozawa K, Shiomi D, Nakazawa Y, Ishikawa M, Takahashi M, Awaga K, Inabe T, Maruyama Y (1991) Chem Lett 1225
59. Takahashi M, Turek P, Nakazawa Y, Tamura M, Nozawa K, Shiomi D, Ishikawa M, Kinoshita M (1991) Phys Rev Lett 67:746
60. Tamura M, Nakazawa Y, Shiomi D, Nozawa K, Hosokoshi Y, Ishikawa M, Kinoshita M (1991) Chem Phys Lett 186:401

61. Hicks RG (2004) Can J Chem 82:1119
62. Hicks RG, Lemaire MT, Öhrström L, Richardson JF, Thompson LK, Xu Z (2001) J Am Chem Soc 123:7154
63. Maspoch D, Ruiz-Molina D, Wurst K, Domingo N, Cavallini M, Biscarini F, Tejada J, Rovira C, Veciana J (2003) Nat Mater 2:190
64. Cao R, Sun D, Liang Y, Hong M, Tatsumi K, Shi Q (2002) Inorg Chem 41:2087
65. Gilroy JB, Koivisto BD, McDonald R, Ferguson MJ, Hicks RG (2006) J Mater Chem 16:2618
66. Kahn O (1993) Molecular magnetism. VCH, New York
67. Fegy K, Luneau D, Ohm T, Paulsen C, Rey P (1998) Angew Chem Int Ed 37(9):1270
68. Miller JS, Zhang JH, Reiff WM, Preston LD, Reis AH Jr, Gerbert E, Extine M, Troup J, Ward MD (1987) J Phys Chem 91:4344
69. Manriquez JM, Yee GT, McLean RS, Epstein AJ, Miller JS (1991) Science 252:1415
70. Miller JS, Calabrese JC, Epstein AJ, Bigelow RW, Zhang JH, Reiff WM (1986) J Chem Soc, Chem Commun 1026
71. Sato O, Cui A, Matsuda R, Tao J, Hayami S (2007) Acc Chem Res 40:361
72. Maspoch D, Ruiz-Molina D, Wurst K, Rovira C, Veciana J (2002) Chem Commun 2958
73. Maspoch D, Ruiz-Molina D, Wurst K, Vidal-Gancedo J, Rovira C, Veciana J (2004) Dalton Trans 1073
74. Maspoch D, Domingo N, Ruiz-Molina D, Wurst K, Hernández JM, Lloret F, Tejada J, Rovira C, Veciana J (2007) Inorg Chem 46:5
75. Maspoch D, Domingo N, Ruiz-Molina D, Wurst K, Tejada J, Rovira C, Veciana J (2004) J Am Chem Soc 126:730
76. Roques N, Maspoch D, Wurst K, Ruiz-Molina D, Rovira C, Veciana J (2006) Chem Eur J 12:9238
77. Wang Z, Zhang T, Otsuka T, Inoue K, Kobayashi H, Kurmoo M (2004) Dalton Trans 2209
78. Wang X-Y, Gan L, Zhang S-W, Gao S (2004) Inorg Chem 43:4615
79. Viertelhaus M, Adler P, Clérac R, Anson CE, Powell AK (2005) Eur J Inorg Chem 692
80. Rettig SJ, Thompson RC, Trotter J, Xia S (1999) Inorg Chem 44:572
81. Wang X-Y, Wei H-Y, Wang Z-M, Chen Z-D, Gao S (2005) Inorg Chem 44:572
82. Wang Z, Zhang B, Fujiwara H, Kobayashi H, Kurmoo M (2004) Chem Commun 416
83. Cornia A, Caneschi A, Dapporto P, Fabretti AC, Gatteschi D, Malavasi W, Sangregorio C, Sessoli R (1999) Angew Chem Int Ed 38:1780
84. Decurtins S, Pellaux R, Antonerra G, Palacio F (1999) Coord Chem Rev 192:841
85. Nikolaï SI, Makhaev VD, Aldoshin SM, Gredin P, Boubekeur K, Train C, Gruselle M (2005) Dalton Trans 3101
86. Gruselle M, Thouvenot R, Malézieux B, Train C, Gredin P, Demeschik TV, Troitskaya LL, Sokolov VI (2004) Chem Eur J 10:4763
87. Coronado E, Galán-Mascaros JR, Gómez-Garcia CJ, Ensling J, Gütlich P (2000) Chem Eur J 6:552
88. Coronado E, Galán-Mascaros JR, Gómez-Garcia CJ, Martínez-Agudo JM (1999) Adv Mater 11:558
89. Larionova J, Mombelli B, Sanchiz J, Kahn O (1998) Inorg Chem 37:679
90. Clemente-León M, Coronado E, Galán-Mascaros JR, Gómez-Garcia CJ (1997) Chem Commun 1727
91. Mathonière C, Carling SG, Yusheng D, Day P (1994) J Chem Soc, Chem Commun 1551
92. Tamaki H, Zhong ZJ, Matsumoto N, Kida S, Koikawa M, Achiwa N, Hashimoto Y, Okawa H (1992) J Am Chem Soc 114:6974
93. Andrés R, Brissard M, Gruselle M, Train C, Vaisserman J, Malézieux B, Jamet J-P, Verdaguer M (2001) Inorg Chem 40:4633
94. Coronado E, Galán-Mascaros JR, Gómez-Garcia CJ, Martínez-Agudo JM (2001) Inorg Chem 40:113
95. Sieber R, Descurtins S, Stoeckli-Evans H, Wilson C, Yufit D, Howard JAK, Capelli SC, Hauser A (2000) Chem Eur J 6:361

96. Lancaster T, Blundell SJ, Pratt FL, Coronado E, Galán-Mascaros JR (2004) J Mater Chem 14:1518
97. Nuttall CJ, Day P (1998) Chem Mater 10:3050
98. Pellaux R, Schmalle HW, Huber R, Fischer P, Hauss T, Ouladdiaf B, Descurtins S (1997) Inorg Chem 36:2301
99. Descurtins S, Schmalle HW, Pellaux R, Huber R, Fischer P, Ouladdiaf B (1996) Adv Mater 8:647
100. Farrel RP, Hambley TW, Lay PA (2004) Inorg Chem 126:32
101. Gruselle M, Train C, Boubekeur K, Gredin P, Ovanesyan N (2006) Coord Chem Rev 250:2491
102. Pointillart T, Gruselle M, Andre G, Train C (2008) J Phys Cond Matter 20:135214
103. Coronado E, Galán-Mascaros JR (2005) J Mater Chem 15:66
104. Coronado E, Day P (2004) Chem Rev 104:5419
105. Coronado E, Galán-Mascaros JR, Gómez-Garcia CJ, Laukhin V (2000) Nature 408:447
106. Lu JY, Lawandy MA, Li J, Yuen T, Lin CL (1999) Inorg Chem 38:2695
107. Yuen T, Lin CL, Mihalisin TW, Lawandy MA, Li J (2000) J Appl Phys 87:6001
108. Armentano D, De Munno G, Lloret F, Palii AV, Julve M (2002) Inorg Chem 41:2007
109. Armentano D, De Munno G, Mastropietro TF, Julve M, Lloret F (2005) J Am Chem Soc 127:10778
110. Pei Y, Journaux Y, Kahn O, Dei A, Gatteschi D (1986) J Chem Soc, Chem Commun 1300
111. Ribas J, Díaz C, Costa R, Journaux Y, Mathonière C, Kahn O, Gleizes A (1990) Inorg Chem 29:2042
112. Vicente R, Escuer A, Ribas J (1992) Polyhedron 11:857
113. Ribas J, Diaz C, Solans X, Font-Badia M (1997) J Chem Soc, Dalton Trans 35
114. Fettouhi M, Ouahab L, Boukhari A, Cador O, Mathonière C, Kahn O (1996) Inorg Chem 35:4932
115. Pereira CLM, Pedroso EF, Novak MA, Brandl AL, Knobel M, Stumpf HO (2003) Polyhedron 22:2387
116. Stumpf HO, Pei Y, Kahn O, Sletten J, Renard J-P (1993) J Am Chem Soc 115:6738
117. Kadam RM, Bhide MK, Sastry MD, Yakhmi JV, Kahn O (2002) Chem Phys Lett 357:457
118. Vaz MGF, Ardisson JD, Speziali NL, Souza GP, Stumpf HO, Knobel M, Macedo WAA (2001) Polyhedron 20:1431
119. Stumpf HO, Ouahab L, Pei Y, Grandjean D, Kahn O (1993) Science 261:447
120. Stumpf HO, Ouahab L, Pei Y, Bergerat P, Kahn O (1994) J Am Chem Soc 116:3866
121. Stumpf HO, Pei Y, Michaut O, Kahn O, Renard JP, Ouahab L (1994) Chem Mater 6:257
122. Cador O, Price D, Larionova J, Mathonière C, Kahn O, Yakhmi J V (1997) Inorg Chem 7:1263
123. Pardo E, Ruiz-Garcia R, Cano J, Ottenwaelder X, Lescouëzec R, Journaux Y, Lloret F, Julve M (2008) DaltonTrans 2780
124. Pereira CLM, Pedroso E, Stumpf HO, Novak MA, Ricard L, Ruiz-García R, Rivière E, Journaux Y (2004) Angew Chem Int Ed 43:955
125. Pardo E, Cangussu D, Dul M-C, Lescouëzec R, Herson P, Journaux Y, Pedroso EF, Pereira CLM, Muñoz M-C, Ruiz-García R, Cano J, Amorós P, Julve M, Lloret F (2008) Angew Chem Int Ed 47:4211
126. Maji TK, Sain S, Mostafa G, Lu T-H, Ribas J, Montfort M, Chaudhuri NR (2003) Inorg Chem 42:709
127. Sain S, Maji TK, Mostafa G, Lu T-H, Chaudhuri NR (2003) New J Chem 27:185
128. Delgado FS, Sanchiz J, Ruiz-Pérez C, Lloret C, Julve M (2003) Inorg Chem 42:5938
129. Konar S, Mukherjee PS, Drew MGB, Ribas J, Chaudhuri NR (2003) Inorg Chem 42:2545
130. Long LS, Chen X-M, Tong M-L, Sun Z-G, Ren Y-P, Huang R-B, Zheng L-S (2001) J Chem Soc, Dalton Trans 1888
131. Zheng Y-Q, Lin J-L, Kong Z-P (2004) Inorg Chem 43:2590
132. Lee E, Kim Y, Jung D-Y (2002) Inorg Chem 41:501
133. Liu T-F, Sun H-L, Gao S, Zhang SW, Lau T-C (2003) Inorg Chem 42:4792
134. Forster PM, Cheetham AK (2003) Angew Chem Int Ed 41:457

135. Guillou N, Livage C, Drillon M, Férey G (2003) Angew Chem Int Ed 42:5314
136. Guillou N, Livage C, van Beek W, Nogués M, Férey G (2003) Angew Chem Int Ed 42:644
137. Miyasaka H, Nakata K, Lecren L, Coulon C, Nakasawa Y, Fujisaki T, Sugiura K, Yamashita M, Clérac R (2006) J Am Chem Soc 128:3770
138. Murugesu M, Wernsdorfer W, Abboud KA, Brechin EK, Christou G (2006) Dalton Trans 2285
139. Wittick LM, Murray KS, Moubaraki B, Batten SR, Spiccia L, Berry KJ (2004) Dalton Trans 1003
140. Moushi EE, Stamatatos TC, Wernsdorfer W, Nastopoulos V, Christou G, Tasiopoulos AJ (2006) Angew Chem Int Ed 45:7722
141. Zheng X-J, Jin K-P, Gao S (2004) Inorg Chem 43:1600
142. Lin WB, Evans OR, Yee GT (2000) J Solid State Chem 152:152
143. Ovcharenko V, Fursova E, Romanenko G, Ivorskii V (2004) Inorg Chem 43:3332
144. Chiang R-K, Chuang N-T, Wur C-S, Chong M-F, Lin C-R (2002) J Solid State Chem 166:158
145. Ma B-Q, Zhang D-S, Gao S, Jin T-Z, Yan C-H, Xu G-X (2000) Angew Chem Int Ed 39:3644
146. Cheng J-W, Zheng S-T, Liu W, Yang G-Y (2008) CrystEngComm 10:1047
147. Xiang S, Wu X, Zhang J, Fu R, Hu S, Zhang X (2005) J Am Chem Soc 127:16352
148. Barthelet K, Riou D, Férey G (2002) Chem Commun 1492
149. Chui SS-Y, Lo SM-F, Charmant JPH, Orpen AG, Williams ID (1999) Science 283:1148
150. Zhang XX, Chui SS-Y, Williams ID (2000) J Appl Phys 87:6007
151. Moulton B, Lu J, Hajndl R, Hariharan S, Zaworotko MJ (2002) Angew Chem Int Ed 41:2821
152. Atwood JL (2002) Nat Mater 1:91
153. Bourne SA, Lu J, Mondal A, Moulton B, Zaworotko MJ (2001) Angew Chem Int Ed 40:11
154. Srikanth H, Hajndl R, Moulton B, Zaworotko M (2003) J Appl Phys 93:7089
155. Chen B, Eddaoudi M, Reineke TM, Kampf W, O'Keefe M, Yaghi OM (2000) J Am Chem Soc 122:11559
156. Cao R, Shi Q, Sun D, Hong M, Bi W, Zhao Y (2002) Inorg Chem 41:6161
157. Garcia-Terán J-P, Castillo O, Luque A, García-Couceiro U, Román P, Lezama L (2004) Inorg Chem 43:4549
158. Li Y, Hao N, Lu Y, Wang E, Kang Z, Hu C (2003) Inorg Chem 42:3119
159. Zheng Y-Q, Lin J-L, Kong Z-P (2004) Inorg Chem 43:2590
160. Liu Y-H, Tsai H-L, Lu Y-L, Wen Y-S, Wang J-C, Lu K-L (2001) Inorg Chem 40:6426
161. Choi HJ, Suh MP (1998) J Am Chem Soc 120:10622
162. Wang X-Y, Sevov SC (2008) Inorg Chem 47:1037 and references cited therein
163. Livage C, Guillou N, Marrot J, Férey G (2001) Chem Mater 13:4387
164. Zhang L-J, Xu J-Q, Shi Z, Zhao X-L, Wang T-G (2003) J Solid State Chem 32:32
165. Choi HJ, Dinca M, Long JR (2008) J Am Chem Soc 130:7848
166. Halder GJ, Kepert CJ, Moubaraki B, Murray KS, Cashion JD (2002) Science 298:1762
167. Real JA, Andres E, Muñoz MC, Julve M, Granier T, Bousseksou A, Varret F (1995) Science 268:265
168. Tian YQ, Cai C-X, Ren X-M, Duan C-Y, Xu Y, Gao S, You X-Z (2003) Chem Eur J 9:5673
169. Masciocchi N, Galli S, Sironi A, Barea E, Navarro JAR, Salas JM, Tabares LC (2003) Chem Mater 15:2153
170. Barea E, Navarro JAR, Salas JM, Masciocchi N, Galli S, Sironi A (2004) Inorg Chem 43:473
171. Masciocchi N, Galli S, Sironi A, Cariati E, Galindi MA, Barea E, Romero MA, Salas JM, Navarro JAR, Santoyo-González F (2006) Inorg Chem 45:7612
172. Pedireddi VR, Varughese S (2004) Inorg Chem 43:450
173. Wang X-Y, Wang Z-M, Gao S (2007) Chem Commun 1127

174. Habib HA, Sanchiz J, Janiak C (2008) Dalton Trans 1734
175. Wang YL, Yuan D-Q, Bi W-H, Li X, Li X-J, Li F, Cao R (2005) Cryst Growth Des 5:1849
176. Zheng Y-Q, Kong Z-P (2003) Anorg Allg Chem 629:1469
177. Konar S, Corbella M, Zangrado E, Ribas J, Chaudhuri NR (2003) Chem Commun 1424
178. Greve J, Jeß I, Näther C (2003) J Solid State Chem 175:328
179. Caneschi A, Gatteschi D, Laugier J, Rey P (1987) J Am Chem Soc 109:2191
180. Roques N, Maspoch D, Luis F, Camón A, Wurst K, Datcu A, Rovira C, Ruiz-Molina D, Veciana J (2008) J Mater Chem 18:98
181. Ballester M (1985) Acc Chem Res 12:1380
182. Maspoch D, Ruiz-Molina D, Wurst K, Rovira C, Veciana J (2004) Dalton Trans 1073
183. Maspoch D, Domingo N, Ruiz-Molina D, Hernández JM, Lloret F, Tejada J, Rovira C, Veciana J (2007) Inorg Chem 46:1627
184. Maspoch D, Ruiz-Molina D, Wurst K, Rovira C, Veciana J (2004) Chem Commun 1164
185. Maspoch D, Domingo N, Ruiz-Molina D, Wurst K, Tejada J, Rovira C, Veciana J (2005) Chem Commun 5035
186. Roques N, Maspoch D, Imaz I, Datcu A, Sutter J-P, Rovira C, Veciana J (2008) Chem Commun 3160
187. Kitagawa S, Kondo M (1997) Angew Chem Int Ed Engl 36:1725
188. Kitagawa S, Uemura K (2005) Chem Soc Rev 34:109
189. Nakatani K, Carriat JY, Journaux Y, Kahn O, Loret F, Renard JP, Pei Y, Sletten J, Verdaguer M (1989) J Am Chem Soc 111:5739
190. Turner S, Kahn O, Rabardel L (1996) J Am Chem Soc 118:6428
191. Kahn O, Larionova J, Yakhmi JV (1999) Chem Eur J 5:3343
192. Larionova J, Chavan SA, Yakhmi JV, Frøystein AG, Sletten J, Sourisseau C, Kahn O (1997) Inorg Chem 36:6374
193. Férey G (2003) Nature Mater 2:136
194. Kurmoo M, Kumagai H, Chapman KW, Kepert CJ (2005) Chem Commun 3012
195. Kurmoo M, Kumagai H, Akita-Tanaka M, Inoue K, Takagi S (2006) Inorg Chem 45:1627
196. Wang Z, Zhang Y, Liu T, Kurmoo M, Gao S (2007) Adv Funct Mater 17:1523
197. Zhang B, Wang Z, Kurmoo M, Gao S, Inoue K, Kobayashi H (2007) Adv Funct Mater 17:577
198. Dunbar K, Heintz RA (1997) Prog Inor Chem 45:283
199. Verdaguer M, Bleuzen A, Marvaud V, Vaisserman J, Seuleima M, Desplanches C, Scuiller A, Train C, Garde R, Gelly G, Lomenech C, Rosenman I, Veillet P, Cartier C, Villain F (1999) Coord Chem Rev 190–192:1023
200. Larionova J, Kahn O, Golhen S, Ouahab L, Clérac R (1999) J Am Chem Soc 121:3349
201. Larionova J, Clérac R, Sanchiz J, Kahn O, Golhen S, Ouahab L (1998) J Am Chem Soc 120:13088
202. Yanai N, Kaneko W, Yoneda K, Ohba M, Kitagawa S (2007) J Am Chem Soc 129:3496
203. Ohkoshi SI, Arai KI, Sato Y, Hashimoto K (2004) Nat Mater 3:857
204. Milon J, Daniel M-C, Kaiba A, Guionneau P, Brandès S, Sutter J-P (2007) J Am Chem Soc 129:13872
205. Neville SM, Moubaraki B, Murray KS, Kepert CJ (2007) Angew Chem Int Ed 46:2059
206. Neville SM, Halder GJ, Chapman KW, Duriska MB, Southon PD, Cashion JD, Létard J-F, Moubaraki B, Murray KS, Kepert CJ (2008) J Am Chem Soc 130:2869
207. Quesada M, De La Peña-O'Shea VA, Aromí G, Geremia S, Massera C, Roubeau O, Gamez P, Reedijk J (2007) Adv Mater 19:1397
208. Bonhommeau S, Molnár G, Galet A, Zwick A, Real JA, Mc Garvey JJ, Bousseksou A (2005) Angew Chem Int Ed 44:4609
209. Niel V, Thompson AL, Muñoz MC, Galet A, Goeta AE, Real JA (2003) Angew Chem Int Ed 42:3760
210. Fu PF, Khan MA, Nicholas KM (1996) J Organomet Chem 506:49
211. Gibson DH, Ye M, Sleadd BA, Mehta JM, Mbadike OP, Richardson JF, Mashuta MS (1995) Organometallics 14:1242

212. Navarro JAR, Barea E, Rodríguez-Diéguez A, Sala JM, Ania CO, Parra JB, Masciocchi N, Galli S, Sironi A (2008) J Am Chem Soc 130:3978
213. Lin C, Kagan CR (2003) J Am Chem Soc 125:336
214. Hermes S, Zacher D, Baunemann A, Wöll C, Fischer RA (2007) Chem Mater 19:2168
215. Shekhah O, Wang H, Strunskus T, Cyganik P, Zacher D, Fischer R, Wöll C (2007) Langmuir 23:7440
216. Shekhah O, Wang H, Kowarik S, Schreiber F, Paulus M, Tolan M, Sternemann C, Evers F, Zacher D, Fischer RA, Wöll C (2007) J Am Chem Soc 129:15118
217. Kosbar L, Srinivasan C, Afzali A, Graham T, Copel M, Krusin-Elbaum L (2006) Langmuir 22:7631
218. Cobo S, Molnár G, Real JA, Bousseksou A (2006) Angew Chem Int Ed 45:5786
219. Molnár G, Cobo S, Real JA, Carcenac F, Daran E, Vieu C, Bousseksou A (2007) Adv Mater 19:2163
220. Shekhah O, Roques N, Mugnaini V, Munuera C, Ocal C, Veciana J, Wöll C (2008) Langmuir 24:6640
221. Lehn J-M (1995) Supramolecular chemistry: concepts and perspectives. VCH, New York
222. Leininger S, Olenyuk B, Stang PJ (2000) Chem Rev 100:853
223. Gianneschi NC, Masar MS III, Mirkin CA (2005) Acc Chem Res 38:825
224. Ono K, Yoshisawa M, Kato T, Watanabe K, Fujita M (2007) Angew Chem Int Ed 46:1803
225. Kuehl CJ, Kryschenko YK, Radhakrishnan U, Seidel SR, Huang SD, Stang PJ (2002) Proc Natl Acad Sci USA 99:4932
226. Yamanoi Y, Sakamoto Y, Kusukawa T, Fujita M, Sakamoto S, Yamaguchi K (2001) J Am Chem Soc 123:980
227. Fujita M, Oguro D, Miyazawa M, Oka H, Yamaguchi K, Ogura K (1995) Nature 378:469
228. Fujita M, Tominaga M, Hori H, Therrien B (2005) Acc Chem Res 38:371
229. Russel S, Seidel SR, Stang PJ (2002) Acc Chem Res 35:972
230. Beer PD, Gale PA (2001) Angew Chem Int Ed 40:486
231. Lützen A (2005) Angew Chem Int Ed 44:1000
232. Hof F, Rebek J Jr (2002) Proc Natl Acad Sci USA 99:4775
233. Pluth MD, Bergman RG, Raymond KN (2007) Science 316:85
234. Company A, Roques N, Güell M, Mugnaini V, Gómez L, Imaz I, Datcu A, Solà M, Luis JM, Veciana J, Ribas X, Costas M (2008) Dalton Trans 1769
235. Nakabayashi K, Ozaki Y, Kawano M, Fujita M (2008) Angew Chem Int Ed 47:2046
236. Harbuzaru BV, Corma A, Rey F, Atienzar P, Jordá JL, García H, Ananias D, Carlos DL, Rocha J (2008) Angew Chem Int Ed 47:1080
237. Liepold L, Anderson S, Willits D, Oltrogge L, Frank JA, Douglas T, Young M (2007) Magn Res Med 58:871
238. Rieter WJ, Taylor KLM, An H, Lin W, Lin W (2006) J Am Chem Soc 128:9024
239. Chelebaeva E, Guari Y, Larionova J, Trifonov A, Guérin C (2008) Chem Mater 20:1367
240. Brinzei D, Catala L, Mathonière C, Wernsdorfer W, Gloter A, Stephan O, Mallah T (2007) J Am Chem Soc 129:3778
241. Imaz I, Maspoch D, Rodríguez-Blanco C, Pérez-Falcón JM, Campo J, Ruiz-Molina D (2008) Angew Chem Int Ed 47:1857
242. Imaz I, Luis F, Carbonera C, Ruiz-Molina D, Maspoch D (2008) Chem Commun 1202
243. Forestier T, Mornet S, Daro N, Nishihara T, Mourib S-I, Tanaka K, Létard J-F (2008) Chem Commun 36:4327
244. Volatron F, Catala L, Rivière E, Gloter A, Stéphan O, Mallah T (2008) Inorg Chem 47:6584
245. Chem Soc Rev (2009) 38: Metal–organic frameworks issue – Reviewing the latest developments across the interdisciplinary area of metal–organic frameworks from an academic and industrial perspective